Toki T, Kanezaki R, Kobayashi E, Kaneko H, Suzuki M, Wang R, Terui K, Kanegane H, Maeda M, Endo M, Mizuochi T, Adachi S, Hayashi Y, Yamamoto M, Shimizu R, Ito E.	Naturally occurring oncogenic GATA1 mutants with internal deletions in transient abnormal myelopoiesis in Down syndrome.	Blood	121	3181-3184	2013
Makishima H, Yoshida K, Nguyen N, Przychodzen B, Sanada M, Okuno Y, Ng KP, Gudmundsson KO, Vishwakarma BA, Jerez A, Gomez-Segui I, Takahashi M, Shiraishi Y, Nagata Y, Guinta K, Mori H, Sekeres MA, Chiba K, Tanaka H, Muramatsu H, Sakaguchi H, Paquette RL, McDevitt MA, Kojima S, Sauntharajah Y, Miyano S, Shih LY, Du Y,Ogawa S, Maciejewski JP.	Somatic SETBP1 mutations in myeloid malignancies.	Nat Genet	45	942-946	2013
Kiyokawa N, Iijima K, Tomita O, Miharu M, Hasegawa D, Kobayashi K, Okita H, Kajiwara M, Shimada H, Inukai T, Makimoto A, Fukushima T, Nanmoku T, Koh K, Manabe A, Kikuchi A, Sugita K, Fujimoto J, Hayashi Y, Ohara A.	Significance of CD66c expression in childhood acute lymphoblastic leukemia.	Leuk Res	38	42-48	2014

Saida S, Watanabe K, Sato-Otsubo A, Terui K, Yoshida K, Okuno Y, Toki T, Wang R, Shiraishi Y, Miyano S, Kato I, Morishima T, Fujino H, Umeda K, Hiramatsu H, Adachi S, Ito E, Ogawa S, Ito M, Nakahata T, Heike T.	Clonal selection in xenografted TAM recapitulates the evolutionary process of myeloid leukemia in Down syndrome.	Blood	121	4377-4387	2013
Hiramoto T, Ebihara Y, Mizoguchi Y, Nakamura K, Yamaguchi K, Ueno K, Nariai N, Mochizuki S, Yamamoto S, Nagasaki M, Furukawa Y, Tani K, Nakauchi H, Kobayashi M, Tsuji K.	Wnt3a stimulates maturation of impaired neutrophils developed from severe congenital neutropenia patient-derived pluripotent stem cells	Proceedings of the National Academy of Sciences of the United States of America	110	3023-3028	2013
Horibe K, Saito AM, Takimoto T, Tsuchida M, Manabe A, Shima M, Ohara A, Mizutani S.	Incidence and survival rates of hematological malignancies in Japanese children and adolescents (2006-2010): based on registry data from the Japanese Society of Pediatric Hematology.	Int J Hematol	98	74-88	2013

Ⅳ. 研究成果の代表的論文

Int J Hematol (2014) 99:154–161
DOI 10.1007/s12185-013-1487-5

ORIGINAL ARTICLE

Liver disease is frequently observed in Down syndrome patients with transient abnormal myelopoiesis

Myoung Ja Park · Manabu Sotomatsu · Kentaro Ohki · Kokoro Arai · Kenichi Maruyama · Tomio Kobayashi · Akira Nishi · Kiyoko Sameshima · Takeshi Takagi · Yasuhide Hayashi

Received: 1 August 2013 / Revised: 26 November 2013 / Accepted: 26 November 2013 / Published online: 14 December 2013

Abstract Transient abnormal myelopoiesis (TAM) in neonates with Down syndrome (DS) is characterized by the transient appearance of blast cells, which resolves spontaneously. Approximately 20 % of patients with TAM die at an early age due to organ failure, including liver disease. We studied 25 DS-TAM patients retrospectively to clarify the correlation between clinical and laboratory characteristics and liver diseases. Early death (<6 months of age) occurred in four of the 25 patients (16.0 %), and two of those four patients died due to liver failure. Although physiologic jaundice improved gradually after a week, all DS patients had elevated D-Bil levels during the clinical course of TAM, except one who suffered early death. The median peak day of the WBC count, total bilirubin (T-Bil) and D-Bil levels was: day 1 (range day 0–57), day 8 (range day 1–55), and day 17 (range 1–53), respectively. Our results reveal that all patients with DS-TAM may develop liver disease irrespective of the absence or presence of symptoms and risk factors for early death. In patients of DS-TAM, careful observation of the level of D-Bil is needed by at least 1 month of age for the detection of liver disease risk.

Keywords Down syndrome · AML · Liver disease · Direct bilirubin · Cytarabine therapy

M. J. Park (✉) · M. Sotomatsu · K. Ohki · K. Arai · Y. Hayashi
Department of Hematology/Oncology, Gunma Children's Medical Center, 779 Shimohakoda, Hokkitsu, Shibukawa, Gunma 377-8577, Japan
e-mail: pakum-tky@umin.ac.jp

K. Maruyama
Department of Neonatology, Gunma Children's Medical Center, Gunma, Japan

T. Kobayashi
Department of Cardiology, Gunma Children's Medical Center, Gunma, Japan

A. Nishi
Department of Pediatric Surgery, Gunma Children's Medical Center, Gunma, Japan

K. Sameshima
Department of Genetics, Gunma Children's Medical Center, Gunma, Japan

T. Takagi
Department of Obstetrics, Gunma Children's Medical Center, Gunma, Japan

Introduction

Down syndrome (DS), or constitutional trisomy 21, is the most common human aneuploidy with an incidence of 1 in 700 births [1]. About 10 % of neonates with DS exhibit unique clonal myeloproliferation characterized by immature megakaryoblasts in the fetal liver and peripheral blood (PB) [2–4]. The first case was reported as transient leukemia, and this hematological abnormality is also known as transient myeloproliferative disorder [5, 6]. In the 2008 version of the World Health Organization classification, it was referred to as myeloid proliferations related to DS, 'transient abnormal myelopoiesis' (TAM) [7, 8]. Although megakaryoblasts spontaneously regress in most patients by the age of 3 months, it is regarded as a pre-leukemic syndrome; approximately 20 % of children diagnosed with TAM develop acute megakaryoblastic leukemia (AMKL) within 4 years [6, 9, 10].

The majority of affected neonates with DS may be asymptomatic other than an elevated WBC count or

hepatomegaly [11, 12]. TAM infrequently presents as hydrops fetalis in utero, but is commonly diagnosed during the first week after birth [12, 13]. Approximately 20 % of TAM patients die at an early age due to organ failure, including liver disease [9, 12, 14]. According to previous reports, early death was correlated with a higher WBC count, ascites, preterm delivery, bleeding diatheses, failure of spontaneous remission, and elevated direct bilirubin (D-Bil) levels [9, 12, 14].

Jaundice, the visible sign of hyperbilirubinemia, is more common in infancy than at any other time of life. Physiologic jaundice is the most common cause of neonatal jaundice. In general, there are some criteria to help distinguish physiologic jaundice from pathologic jaundice in neonates. These included: (1) jaundice prior to 36 h of age, (2) a serum total bilirubin (T-Bil) level above 12 mg/dl, (3) persistent jaundice beyond the eighth day of life, and (4) D-Bil fraction is >2 mg/dl at any time [15, 16].

Cholestasis affects approximately 1 in every 2,500 infants and is an infrequent but potentially serious condition that indicates liver dysfunction [17, 18]. Since hyperbilirubinemia may be present in an infant who does not appear acutely ill, the measurement of D-Bil or conjugated bilirubin level is recommended [19, 20]. The potential cause of cholestasis in neonates is diverse; therefore, it is important to recognize specific treatable metabolic or infectious diseases and establish early, appropriate, and effective management. Every infant presenting with jaundice beyond the age of 2 weeks should be evaluated with fractionated bilirubin to exclude life-threatening conditions or disorders requiring urgent specific treatment [21].

A prospective study reported that 21 % of TAM patients developed the symptoms of cholestasis or elevated liver enzymes [12]. TAM is sometimes complicated by liver fibrosis, which is life-threatening and often fatal [22–25]. However, the precise frequency of liver fibrosis is not known. The infiltration of megakaryoblasts with liver fibrosis has been shown histologically [22, 23]. The DS-TAM patients with liver fibrosis will be progressive and fatal [24, 26].

Elevated D-Bil levels are a sign of serious liver disease in infants with TAM [6]. However, the detailed clinical characteristics of TAM with liver disease remain unclear. We studied 25 DS-TAM patients in our hospital retrospectively to clarify the correlation between clinical and laboratory characteristics and liver diseases.

Methods

A retrospective chart review of patients admitted to Gunma Children's Medical Center in Japan between January 2001 and June 2012 was undertaken to identify the characteristics of liver disease in DS infants with TAM. Morphologic evidence of myeloid blasts in the PB was confirmed in all eligible patients. The eligibility criteria for this analysis were DS infants who were younger than 3 months. Patients with leukocytosis and peripheral blast cells as a result of infections or other causes were excluded. Elevated D-Bil levels were defined as D-Bil level $\geq$ 1.5 mg/dl [15, 16, 20]. Here we defined conjugated hyperbilirubinemia as D-Bil $\geq$ 2 mg/dl. Although the terms D-Bil are used equivalently with conjugated bilirubin in the reviews [16], this is no quantitatively correct, because the direct fraction includes both conjugated bilirubin and delta bilirubin [19]. It has been reported that the 99th percentile for D-Bil is 2.1 mg/dl in the retrospective study of a birth cohort of 271,186 full-term newborns including 259 DS infants [27]. D-Bil fraction $\geq$2 mg/dl at any time is pathological jaundice in neonate, whether the patient is Down syndrome or not, that indicates the possibility of cholestasis. Cholestasis is defined physiologically as reduction in bile flow and morphologically as the presence of bile pigment in histologic sections of liver [16]. This study was approved by the Ethics Committee of our hospital, and written informed consent was obtained from all parents.

Results

The clinical characteristics of TAM patients are summarized in Table 1. The 25 patients in this study included 13 males and 12 females. The median gestational age and birth weight were 37 weeks (range 32–41 weeks) and 2,600 g (range 1,622–3,552 g), respectively. The median age at diagnosis was 0 days, with a range from 0 to 28 days. Congenital cardiac abnormalities were seen in 21 (84.0 %) of 25 patients. Elevated D-Bil levels were found in 24 (96.0 %) of 25 patients, systemic edema in 5 (20.0 %) of 25, and disseminated intravascular coagulation (DIC) in 5 (20.0 %) of 25, respectively. Among the 25 patients requiring therapeutic intervention, 6 received exchange blood transfusion, 5 received steroid therapy, and 3 received a low dose of cytarabine. Early death (<6 months of age) occurred in 4 (16.0 %) of 25 patients and the median age at death was 50 days (range 1–156 days). Two of the 4 patients were born with hydrops fetalis and died at day 1 and 44 due to multiorgan failure. The other 2 patients died because of liver failure. Six patients (24.0 %) developed AMKL.

The laboratory findings of 25 patients are summarized in Table 2. The median WBC count and percentage of blasts in the PB at diagnosis were 30,600/μl (range 4,600–183,000/μl) and 36 % (range 2–96 %), respectively. The median peak day of the WBC count, and T-Bil and

Table 1 Clinical findings in 25 TAM cases

Patient number	Gender	Gestational age (weeks)	Birth weight (g)	Age at diagnosis (day)	Congenital abnormalies	Cholestatic jaundice	Systemic edema	DIC	Therapeutic intervention	Outcome	AMKL
1	F	35	2,710	0	VSD	−	+	+	−	Dead at day 1	−
2	M	37	2,958	0	PDA, ASD, VSD	+	+	−	PSL, ET, AraC	Alive	−
3	M	40	3,552	0	PDA, ASD, VSD	+	−	+	PSL	Dead at day 609	−
4	F	39	2,884	0	PDA, ASD, VSD	+	−	−	−	Alive	−
5	F	37	2,870	0	PDA, ASD, VSD	+	−	+	ET	Alive	+
6	M	35	2,680	16	PDA, ASD, VSD	+	−	−	−	Alive	−
7	M	38	2,600	0	VSD	+	−	−	−	Alive	−
8	M	38	3,282	0	PDA	+	−	+	−	Dead at day 1,217	+
9	M	37	2,252	25	−	+	−	−	PSL, ET, AraC	Dead at day 156	−
10	M	34	2,038	28	PDA, TOF	+	−	−	−	Alive	−
11	F	38	2,626	7	PDA	+	−	−	−	Alive	−
12	F	32	1,622	0	−	+	−	−	−	Alive	+
13	F	32	2,122	0	ASD	+	+	−	−	Dead at 399	−
14	F	34	2,510	21	PDA, ASD	+	+	−	ET	Dead at day 44	−
15	M	36	2,128	0	PDA, ASD	+	−	−	−	Alive	+
16	F	36	2,150	0	−	+	+	+	PSL, ET	Dead at day 55	−
17	F	36	2,059	0	ASD,VSD	+	−	−	−	Alive	−
18	M	41	2,726	0	ASD, VSD	+	−	−	PSL, ET, AraC	Alive	−
19	M	39	2,515	0	ASD, VSD	+	−	−	−	Alive	−
20	M	35	2,890	1	−	+	−	−	−	Alive	−
21	F	36	1,992	3	PDA, VSD	+	−	−	−	Alive	+
22	F	37	2,802	0	ASD, VSD, TOF	+	−	−	−	Alive	−
23	M	34	2,058	3	PDA	+	−	−	−	Alive	+
24	F	37	2,554	0	PDA, VSD	+	−	−	−	Alive	−
25	M	39	2,870	8	PDA	+	−	−	−	Alive	−

ASD atrial septal defect, *VSD* ventricular septal defec, *TOF* tetralogy of Fallot, *PDA* patent ductus arteriosus, *PSL* prednisolone, *ET* exchange blood transfusion, *AraC* cytarabine

D-Bil levels were day 1 (range day 0–57), day 8 (range day 1–55), and day 17 (range 1–53), respectively. All 24 patients except one suffered from early death showed D-Bil levels above 1.5 mg/dl, and 19 (76.0 %) of 25 patients showed D-Bil levels above 2.0 mg/dl with or without the symptoms of liver failure. The median first day of D-Bil levels over 1.5 and 2.0 mg/dl was day 10 (range day 1–28) and day 14 (range day 0–32), respectively. Liver biopsy was performed in 3 patients with the symptoms of liver failure. The pathological diagnosis of patient 6 was non-syndromic paucity of interlobular bile ducts (NS-PILBD).

The correlation between patient covariates and conjugated hyperbilirubinemia (D-Bil $\geq$ 2 mg/dl) is shown in Table 3. Conjugated hyperbilirubinemia was not significantly associated with gender, birth weight, gestational age, DIC, systemic edema, or a higher WBC count. The

Table 2 Laboratory findings in 25 TAM cases

Patient number	WBC count at diagnosis (/μl)	PB blasts (%)	Platelet ($\times 10^3$/μl)	Peak value of WBC (/μl)	Day of peak WBC	Peak value of T-Bil (mg/dL)	Day of peak T-Bil	Peak value of D-Bil (mg/dL)	Day of peak D-Bil	Day of D-Bil ≥2 mg/dl	Day of D-Bil ≥1.5 mg/dl	Peak value of AST	Peak value of ALT
1	21,300	15	147.0	21,300	0	2.13	1	0.83	1	–	–	254	88
2	12,900	11	210.0	15,300	0	16.32	8	9.47	31	8	2	116	96
3	72,600	53	26.0	72,600	0	12.56	6	2.28	13	13	10	73	126
4	89,400	64	429.0	89,400	0	26.84	11	3.08	23	12	12	102	163
5	183,000	88	665.0	183,000	0	7.12	3	3.14	4	3	1	265	67
6	12,000	4	178.0	13,000	0	23.76	16	6.46	34	16	16	430	374
7	14,500	39	66.0	21,800	2	5.62	3	1.61	1	–	1	50	10
8	74,100	36	162.0	91,200	1	16.33	6	2.36	1	1	1	45	34
9	7,700	22	56.0	7,700	25	29.50	43	18.98	42	25	25	303	125
10	17,200	40	79.0	40,100	57	7.83	28	2.4	29	29	28	48	18
11	30,700	77	83.0	31,900	15	12.28	8	2.4	15	15	15	22	14
12	25,000	50	136.0	25,000	0	12.31	9	3.93	14	14	14	66	24
13	26,000	49	121.0	35,100	1	13.36	9	2.1	4	4	4	785	183
14	114,000	96	4.7	138,000	42	6.49	36	5.97	42	24	24	121	24
15	181,900	87	925.0	183,000	2	12.60	2	1.73	5	–	0	136	179
16	46,200	53	293.0	74,400	21	46.97	55	18.72	53	2	2	214	71
17	32,300	22	59.0	32,300	0	12.56	6	2.8	20	15	1	43	50
18	118,900	89	310.0	118,900	0	13.20	5	3.18	32	32	18	28	21
19	19,500	4	230.0	23,200	2	15.23	2	4.18	10	4	0	105	97
20	41,800	30	241.0	48,900	2	4.10	16	1.92	17	–	4	37	46
21	6,400	6	66.0	10,300	3	13.26	7	2.14	15	15	1	70	76
22	16,400	9	250.0	23,000	1	13.63	6	1.85	14	–	14	39	16
23	36,700	32	960.0	36,700	0	16.18	16	2.12	27	27	27	50	83
24	30,600	6	36.0	35,000	1	17.75	9	1.96	20	–	20	37	10
25	4,600	2	69.0	6,800	46	10.13	8	2.62	20	11	10	88	18

WBC white blood cell, *PB* peripheral blood, *T-Bil* total bilirubin, *D-Bil* direct bilirubin

correlation between patient covariates and early death is shown in Table 4. Early death was significantly associated with a peak D-Bil level of greater than 5 mg/dl ($p = 0.016$).

Five representative patients with marked cholestatic jaundice are described below. The T-Bil and D-Bil levels, WBC count, and blast ratio in the PB of 4 patients are shown in Fig. 1. Figure 1a shows the clinical course of patient 2. He exhibited hydrops fetalis at birth. T-Bil and D-Bil levels at birth were 5.99 and 1.07 mg/dl, respectively. His serum markers of liver fibrosis were high: procollagen Type III Peptide (P-III-P) was 9.7 U/ml (normal range 0.3–0.8 U/ml) and type IV collagen was 1,019 ng/ml (normal range <150 ng/ml). D-Bil levels over 1.5 and 2.0 mg/dl occurred on day 2 and day 8, respectively. After 1 week, the D-Bil level gradually increased while the T-Bil level concomitantly decreased. Although therapeutic intervention was started with steroids and a low dose of cytarabine, the D-Bil level still increased. A liver biopsy was performed to clarify the cause of pathological jaundice. The histopathological findings were mild liver fibrosis without leukemic cell infiltration. After exchange blood transfusion was performed on day 40, pathological jaundice improved.

Patient 9 was admitted to our hospital on day 25 because of jaundice. T-Bil and D-Bil levels at diagnosis were 19.76 and 13.11 mg/dl, respectively. After admission, T-Bil and D-Bil levels gradually increased. Despite therapeutic intervention by exchange blood transfusion, steroids, and a low dose of cytarabine, the patient died on day 156 because of liver failure. Although he received the operation for imperforate anus on day 1, TAM was not diagnosed. The WBC count on day 1 in previous hospital was 7,400/μl and blast in PB was not noticed.

Patient 16 was admitted on day 0 because of congenital jejunal atresia. T-Bil and D-Bil levels at diagnosis were 9.14 and 2.04 mg/dl, respectively. After jejunostomy, the D-Bil level decreased to below normal levels, and then gradually increased again in spite of therapeutic intervention by exchange blood transfusion. The patient died on day 55 because of liver failure. Liver histology showed severe liver fibrosis without leukemic cell infiltration.

Patient 17 was admitted to our hospital because of congenital heart disease. Initial T-Bil and D-Bil levels were

Table 3 Correlation between patient covariates and conjugated hyperbilirubinemia (D-Bil ≧ 2 mg/dl)

	Patients with conjugated hyperbilirubinemia	Patients without conjugated hyperbilirubinemia	Total patients	*p*
Gender				
Male	10	3	13	1
Female	9	3	12	
Birth weight				
Birth weight ≧2.5 kg	11	5	16	0.364
Birth weight <2.5 kg	8	1	9	
Gestational age				
Term ≧37 weeks	10	3	13	1
Preterm <37	9	3	12	
Systemic edema				
+	4	1	5	1
−	15	5	20	
DIC				
+	4	1	5	1
−	15	5	20	
WBC at diagnosis				
WBC ≧10 × 10^4/μl	3	1	4	1
WBC <10 × 10^4/μl	16	5	21	

p value (Fisher's test)

Table 4 Correlation between clinical data and early death

	Patients with EA	Patients without EA	Total patients	*p*
Gender				
Male	1	12	13	0.322
Female	3	9	12	
Birth weight				
Birth weight ≧2.5 kg	2	14	16	0.602
Birth weight <2.5 kg	2	7	9	
Gestational age				
Term ≧37 weeks	1	12	13	0.322
Preterm <37 weeks	3	9	12	
WBC at diagnosis				
WBC ≧100 × 10^3/μl	1	3	4	0.527
WBC <100 × 10^3/μl	3	18	21	
Peak value of D-Bil				
D-Bil ≧5 mg/dl	3	2	5	0.016
D-Bil <5 mg/dl	1	19	20	

EA early death (<6 months of age), *p* value (Fisher's test)

2.34 and 0.87 mg/dl, respectively. The D-Bil level gradually increased from day 15, while the T-Bil level adversely decreased. Megakaryoblasts regressed spontaneously on day 13 and the D-Bil level decreased from day 24 without therapeutic intervention. Her serum markers of liver fibrosis were high from birth: P-III-P was 8.1 U/ml and type IV collagen was 1,040 ng/ml. In this patient, the D-Bil level was above 2 mg/dl and high levels of P-III-P and type IV collagen were observed, but cholestatic symptoms were not apparent.

Patient 19 was admitted to our hospital because of congenital heart disease. Initial T-Bil and D-Bil levels were 5.47 and 1.97 mg/dl, respectively. The level of D-Bil increased from day 4, while the T-Bil level adversely decreased. Therapeutic intervention by steroids was started on day 30. Thereafter, the D-Bil level decreased, and banding therapy for patent ductus arteriosus (PDA) was performed on day 50. Her serum markers of liver fibrosis were P-III-P (17.5 U/ml) and type IV collagen (948 ng/ml).

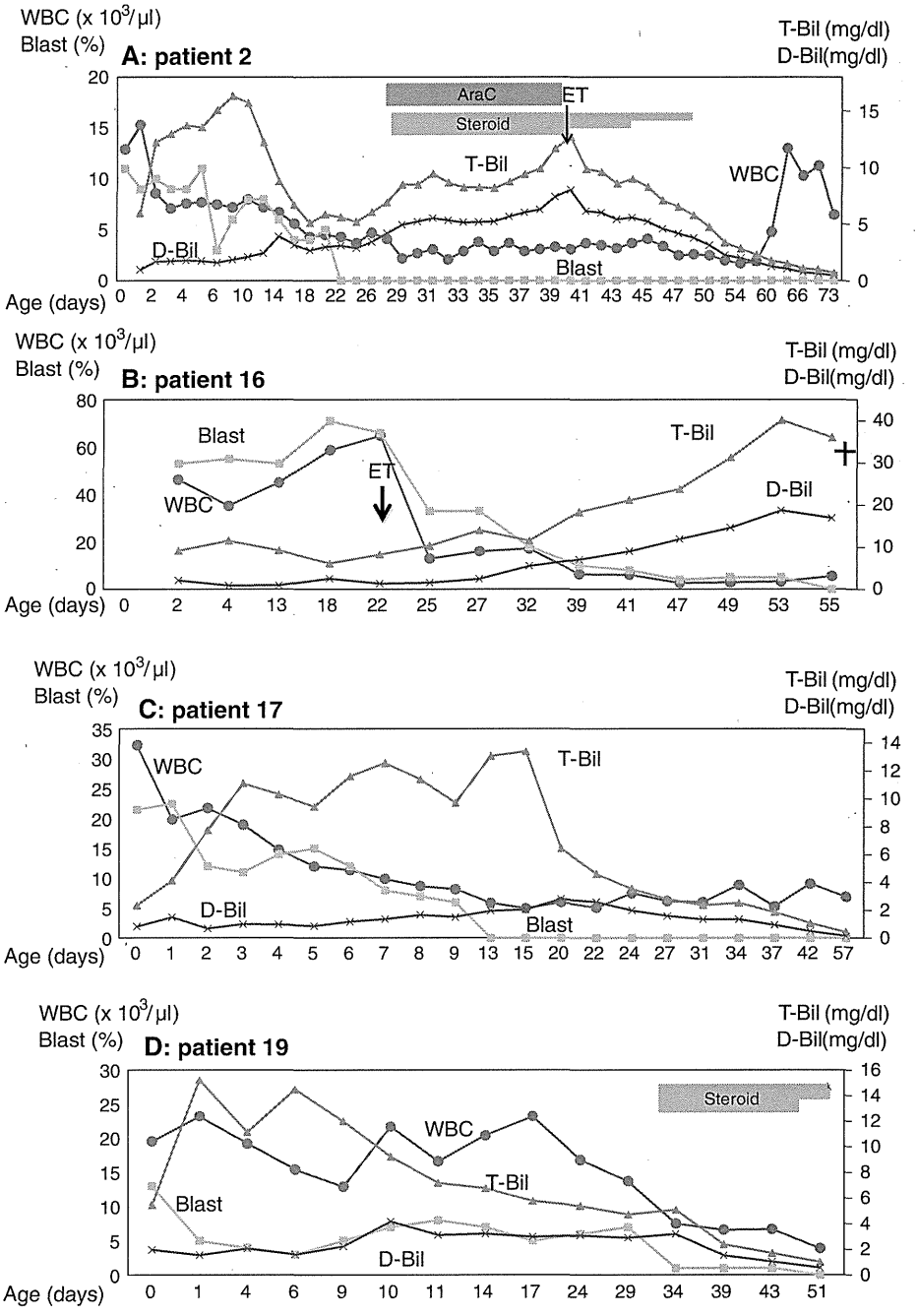

Fig. 1 T-Bil and D-Bil levels, WBC count, and blast ratio in PB of 4 patients (**a** patient 2, **b** patient 16, **c** patient 17, **d** patient 19). *ET* exchange blood transfusion

Discussion

We studied 25 DS-TAM patients retrospectively to clarify the correlation between clinical and laboratory characteristics and liver diseases. Two of 4 patients died within 6 months after birth due to liver failure. Three of 5 patients with D-Bil levels greater than 5 mg/dl died early due to multiorgan failure. Early death was associated with a peak D-Bil level greater than 5 mg/dl ($p = 0.016$). Our result was similar to previous studies [9, 12, 14], but the number of our study was small.

Although our study is retrospective in single institution, we showed that liver disease could occur in DS patients without any risk factor of early death even after the disappearance or decrease of blast cells in PB. In our study, the median first day of D-Bil levels over 1.5 mg/dl and 2.0 mg/dl was day 10 (range day 1–28) and day 14 (range day 0–32), respectively. Although physiologic jaundice improved gradually 1 week after birth, the level of D-Bil adversely increased in all DS patients with TAM. All DS patients had elevated D-Bil levels regardless of the risk for early death during the clinical course of TAM. The level of

D-Bil is one of the most reliable markers in TAM accompanied by liver disease. It is necessary to monitor the level of D-Bil in DS-TAM patients, and careful attention is needed not to exceed above 2 mg/dl.

The precise frequency of TAM is unknown because no large population-based study among patients has been carried out to verify it yet [9]. If the diagnosis of TAM has not been made due to the lack of symptoms within 1 week after birth, similar to patient 9, the TAM patients may already have uncorrectable liver disease at presentation. An urgent referral is considered to be necessary for further diagnostic investigations in patients of elevated D-Bil levels as previously reported [28].

Although the clinical manifestations of neonatal cholestasis are usually similar, they may include potentially serious disorders. However, identifying these neonates with cholestasis from lots of patients with physiologic jaundice can be difficult. As shown in patient 2, T-Bil is not a reliable marker of cholestasis. For this reason, conjugated bilirubin and D-Bil levels are often measured. D-Bil measurement estimates the total concentration of the conjugated and delta bilirubin. False positive results have been reported to be less likely when using conjugated bilirubin levels than when using D-Bil levels in assessment of the biliary disease in newborn [27]. Conjugated bilirubin and D-Bil level measurement may be the prognostic factors to predict severe liver disease in TAM patients.

Differential diagnoses among biliary atresia, idiopathic neonatal hepatitis, and intrahepatic cholestasis are particularly difficult to make. Liver biopsy provides the highest diagnostic usefulness in neonatal cholestasis [28]. Using liver biopsy, we diagnosed NS-PILBD in a cholestatic patient with TAM [29]. Biliary atresia in a DS patient has also been reported [30]. Liver biopsy may allow the differential diagnosis of cholestasis and provide additional information such as the presence of megakaryoblasts in the liver and the severity of liver fibrosis.

The treatment of liver disease in TAM has not yet been established. Hepatic synthetic dysfunction leads to bleeding and it is important to ascertain the cause of bleeding and management of patients who have TAM with liver disease. Medical management is mainly supportive and aims for optimal growth, development, and the treatment of complications such as fat malabsorption, fat-soluble vitamin deficiencies, cirrhosis, portal hypertension, and liver failure [21]. The administration of vitamin K is needed for the initial treatment of cholestatic infants to prevent hemorrhage. The decreased delivery of bile acids to the proximal intestine leads to the inadequate digestion and absorption of dietary long-chain triglycerides and fat-soluble vitamins. Infant formulas containing medium chain triglycerides (MCTs) provide better energy balance. Ursodeoxycholic acid (20 mg/kg/day) may also be effective in encouraging bile flow and bile drainage [31].

It has been reported that treatment with cytarabine (0.5–1.5 mg/kg) has a beneficial effect on the outcome of TAM with high risk factors for early death [12]. In our study, three of 25 patients were treated with a low dose of cytarabine, and D-Bil and transaminases levels increased after cytarabine therapy in patients 2 and 9. It is not certain whether a low dose of cytarabine is effective in TAM patients with liver dysfunction after the disappearance of blast cells in PB. Liver disease in DS-TAM progresses even if blast cells disappear. No therapy is known to be effective in inhibiting the progression of cholestasis or preventing further hepatocellular damage and cirrhosis. Thus, we emphasize that the early detection of DS-TAM patients with liver disease is very important. As shown in patient 16, the percentage of blasts in PB is not related to liver disease, and careful observation of D-Bil or conjugated bilirubin levels was needed at least 1 month of age in DS-TAM.

Another strategy may be to inhibit fibroblastic proliferation with a biological response modifier such as a steroid. The clinical course of patient 19 suggested that some TAM patients with liver disease may benefit from steroid therapy. Cytokines have been reported to be produced by blast cells such as platelet-derived growth factor and transforming growth factor B, and may play an important role in the progression of cholestasis [32–34]. It has been also reported that blasts and liver tissue from TAM patients with hepatic fibrosis showed a significantly elevated expression of PDGF gene [33]. Some DS-TAM patient with liver disease may improve without therapeutic intervention, as patient 17. Treatment with steroids and exchange blood transfusion may be effective in reducing the cytokine storm before serious liver damage can occur.

In summary, we retrospectively studied 25 DS-TAM patients to identify a correlation between clinical and laboratory characteristics and liver diseases. Our results revealed that all patients with DS-TAM have potential liver disease regardless of the existence of symptoms and risk factors for early death. In patients of DS-TAM, careful observation of the level of D-Bil or conjugated bilirubin is needed at least until 1 month of age for liver disease.

Acknowledgments This work was supported by a grant for Cancer Research, and a grant for Research on Children and Families from the Ministry of Health, Labor, and Welfare of Japan, and a Grant-in-Aid for Scientific Research (B) and (C) and Exploratory Research from the Ministry of Education, Culture, Sports, Science, and Technology of Japan, and a Research grant for Bureau of Gunma Prefectural Hospitals.

References

1. Malinge S, Izraeli S, Crispino JD. Insights into the manifestations, outcomes, and mechanisms of leukemogenesis in Down syndrome. Blood. 2009;113:2619–28.
2. Pine SR, Guo Q, Yin C, Jayabose S, Druschel CM, Sandoval C. Incidence and clinical implications of GATA1 mutations in newborns with Down syndrome. Blood. 2007;110:2128–31.
3. Zipursky A, Brown EJ, Christensen H, Doyle J. Transient myeloproliferative disorder (transient leukemia) and hematologic manifestations of Down syndrome. Clin Lab Med. 1999;19: 157–67.
4. Bajwa RP, Skinner R, Windebank KP, Reid MM. Demographic study of leukaemia presenting within the first 3 months of life in the Northern Health Region of England. J Clin Pathol. 2004;57:186–8.
5. Schunk GJ, Lehman WL. Mongolism and congenital leukemia. J Am Med Assoc. 1954;155:250–1.
6. Lange B. The management of neoplastic disorders of haematopoiesis in children with Down's syndrome. Br J Haematol. 2000;110:512–24.
7. Nagao T, Lampkin BC, Hug G. A neonate with Down's syndrome and transient abnormal myelopoiesis: serial blood and bone marrow studies. Blood. 1970;36:443–7.
8. Vardiman JW, Thiele J, Arber DA, Brunning RD, Borowitz MJ, Porwit A, et al. The 2008 revision of the World Health Organization (WHO) classification of myeloid neoplasms and acute leukemia: rationale and important changes. Blood. 2009;114: 937–51.
9. Massey GV, Zipursky A, Chang MN, Doyle JJ, Nasim S, Taub JW, et al. A prospective study of the natural history of transient leukemia (TL) in neonates with Down syndrome (DS): Children's Oncology Group (COG) study POG-9481. Blood. 2006;107: 4606–13.
10. Homans AC, Verissimo AM, Vlacha V. Transient abnormal myelopoiesis of infancy associated with trisomy 21. Am J Pediatr Hematol Oncol. 1993;15:392–9.
11. Zipursky A. Transient leukaemia—a benign form of leukaemia in newborn infants with trisomy 21. Br J Haematol. 2003;120: 930–8.
12. Klusmann JH, Creutzig U, Zimmermann M, Dworzak M, Jorch N, Langebrake C, et al. Treatment and prognostic impact of transient leukemia in neonates with Down syndrome. Blood. 2008;111:2991–8.
13. Zipursky A, Rose T, Skidmore M, Thorner P, Doyle J. Hydrops fetalis and neonatal leukemia in Down syndrome. Pediatr Hematol Oncol. 1996;13:81–7.
14. Muramatsu H, Kato K, Watanabe N, Matsumoto K, Nakamura T, Horikoshi Y, et al. Risk factors for early death in neonates with Down syndrome and transient leukaemia. Br J Haematol. 2008;142:610–5.
15. Ambalavanan N, Carlo WA. Jaundice and hyperbilirubinemia in the Newborn. In: Kligman RM, Stanton BF, Geme JS, Scgor NF, editors. Nelson textbook of pediatrics. Philadelphia: Elsevier; 2011. p. 603–5.
16. Mathis RK, Andres JM, Walker WA. Liver disease in infants. Part II: hepatic disease states. J Pediatr. 1977;90:864–80.
17. Dick MC, Mowat AP. Hepatitis syndrome in infancy–an epidemiological survey with 10 year follow up. Arch Dis Child. 1985;60:512–6.
18. Balistreri WF. Neonatal cholestasis. J Pediatr. 1985;106:171–84.
19. Brumbaugh D, Mack C. Conjugated hyperbilirubinemia in children. Pediatr Rev. 2012;33:291–302.
20. Moyer V, Freese DK, Whitington PF, Olson AD, Brewer F, Colletti RB, et al. Guideline for the evaluation of cholestatic jaundice in infants: recommendations of the North American Society for Pediatric Gastroenterology, Hepatology and Nutrition. J Pediatr Gastroenterol Nutr. 2004;39:115–28.
21. McKiernan PJ. Neonatal cholestasis. Semin Neonatol. 2002;7: 153–65.
22. Becroft DM, Zwi LJ. Perinatal visceral fibrosis accompanying the megakaryoblastic leukemoid reaction of Down syndrome. Pediatr Pathol. 1990;10:397–406.
23. Ruchelli ED, Uri A, Dimmick JE, Bove KE, Huff DS, Duncan LM, et al. Severe perinatal liver disease and Down syndrome: an apparent relationship. Hum Pathol. 1991;22:1274–80.
24. Miyauchi J, Ito Y, Kawano T, Tsunematsu Y, Shimizu K. Unusual diffuse liver fibrosis accompanying transient myeloproliferative disorder in Down's syndrome: a report of four autopsy cases and proposal of a hypothesis. Blood. 1992;80:1521–7.
25. Schwab M, Niemeyer C, Schwarzer U. Down syndrome, transient myeloproliferative disorder, and infantile liver fibrosis. Med Pediatr Oncol. 1998;31:159–65.
26. Al-Kasim F, Doyle JJ, Massey GV, Weinstein HJ, Zipursky A. Incidence and treatment of potentially lethal diseases in transient leukemia of Down syndrome: Pediatric Oncology Group Study. J Pediatr Hematol Oncol. 2002;24:9–13.
27. Davis AR, Rosenthal P, Escobar GJ, Newman TB. Interpreting conjugated bilirubin levels in newborns. J Pediatr. 2011; 158(562–5):e1.
28. De Bruyne R, Van Biervliet S, Vande Velde S, Van Winckel M. Clinical practice: neonatal cholestasis. Eur J Pediatr. 2011;170: 279–84.
29. Sotomatsu M, Park MJ, Shimada A, hayashi Y. A case of Down syndrome with transient abnormal myelopoiesis and nonsyndromic paucity of interlobular bile ducts. Jpn J Pediatric Hematol. 2008;22:34–7.
30. Puri P, Guiney EJ. Intrahepatic biliary atresia in Down's syndrome. J Pediatr Surg. 1975;10:423–4.
31. Kelly DA, Davenport M. Current management of biliary atresia. Arch Dis Child. 2007;92:1132–5.
32. Terui T, Niitsu Y, Mahara K, Fujisaki Y, Urushizaki Y, Mogi Y, et al. The production of transforming growth factor-beta in acute megakaryoblastic leukemia and its possible implications in myelofibrosis. Blood. 1990;75:1540–8.
33. Hattori H, Matsuzaki A, Suminoe A, Ihara K, Nakayama H, Hara T. High expression of platelet-derived growth factor and transforming growth factor-beta 1 in blast cells from patients with Down syndrome suffering from transient myeloproliferative disorder and organ fibrosis. Br J Haematol. 2001;115:472–5.
34. Shimada A, Hayashi Y, Ogasawara M, Park MJ, Katoh M, Minakami H, et al. Pro-inflammatory cytokinemia is frequently found in Down syndrome patients with hematological disorders. Leuk Res. 2007;31:1199–203.

nature genetics

The landscape of somatic mutations in Down syndrome–related myeloid disorders

Kenichi Yoshida[1,2,17], Tsutomu Toki[3,17], Yusuke Okuno[1,17], Rika Kanezaki[3], Yuichi Shiraishi[4], Aiko Sato-Otsubo[1,2], Masashi Sanada[1,2], Myoung-ja Park[5], Kiminori Terui[3], Hiromichi Suzuki[1,2], Ayana Kon[1,2], Yasunobu Nagata[1,2], Yusuke Sato[1,2], RuNan Wang[3], Norio Shiba[5], Kenichi Chiba[4], Hiroko Tanaka[6], Asahito Hama[7], Hideki Muramatsu[7], Daisuke Hasegawa[8], Kazuhiro Nakamura[9], Hirokazu Kanegane[10], Keiko Tsukamoto[11], Souichi Adachi[12], Kiyoshi Kawakami[13], Koji Kato[14], Ryosei Nishimura[15], Shai Izraeli[16], Yasuhide Hayashi[5], Satoru Miyano[4,6], Seiji Kojima[7], Etsuro Ito[3,18] & Seishi Ogawa[1,2,18]

Transient abnormal myelopoiesis (TAM) is a myeloid proliferation resembling acute megakaryoblastic leukemia (AMKL), mostly affecting perinatal infants with Down syndrome. Although self-limiting in a majority of cases, TAM may evolve as non-self-limiting AMKL after spontaneous remission (DS-AMKL). Pathogenesis of these Down syndrome–related myeloid disorders is poorly understood, except for *GATA1* mutations found in most cases. Here we report genomic profiling of 41 TAM, 49 DS-AMKL and 19 non-DS-AMKL samples, including whole-genome and/or whole-exome sequencing of 15 TAM and 14 DS-AMKL samples. TAM appears to be caused by a single *GATA1* mutation and constitutive trisomy 21. Subsequent AMKL evolves from a pre-existing TAM clone through the acquisition of additional mutations, with major mutational targets including multiple cohesin components (53%), *CTCF* (20%), and *EZH2*, *KANSL1* and other epigenetic regulators (45%), as well as common signaling pathways, such as the JAK family kinases, *MPL*, *SH2B3* (*LNK*) and multiple RAS pathway genes (47%).

TAM represents a transient proliferation of immature megakaryoblasts that occurs in 5–10% of perinatal infants with Down syndrome[1,2]. Although morphologically indistinguishable from AMKL, TAM is self-limiting in the majority of cases and usually terminates spontaneously within 3–4 months of birth[1]. Hepatic infiltration of myeloid cells is a common finding and can be severe enough to be fatal, owing to hepatic failure, with liver fibrosis occurring in 5–16% of cases[2–4]. Moreover, even when spontaneous remission is achieved, approximately 20–30% of surviving infants develop DS-AMKL years after remission, although some DS-AMKL cases have no documented history of TAM[4]. In contrast to non–Down syndrome–related AMKL (non-DS-AMKL), which generally shows poor prognosis, individuals with DS-AMKL typically have a favorable prognosis. In molecular pathogenesis of these Down syndrome–related myeloid disorders, *GATA1* mutations are detected in virtually all affected infants, suggesting their central role in Down syndrome–related myeloid proliferation[5,6]. However, it is still open to question whether a *GATA1* mutation is sufficient for the development of TAM in individuals with Down syndrome, what is the cellular origin of the subsequent AMKL, whether additional gene mutations are required for progression to AMKL, and, if so, what are their gene targets, although several genes have been reported to be mutated in occasional cases with DS-AMKL, including *JAK1*, *JAK2* and *JAK3* (refs. 7–10), *TP53* (refs. 10,11), *FLT3* (ref. 8) and *MPL*[12]. We reasoned that identifying a comprehensive registry of gene mutations and tracking them at a clonal level using massively parallel sequencing would provide vital information for addressing these questions.

RESULTS

Genomic landscape of Down syndrome–related myeloid neoplasms

We performed whole-genome sequencing of 4 trios consisting of samples from TAM, AMKL and complete remission phases (**Supplementary Figs. 1** and **2** and **Supplementary Table 1**). In total,

[1]Cancer Genomics Project, Graduate School of Medicine, The University of Tokyo, Tokyo, Japan. [2]Department of Pathology and Tumor Biology, Graduate School of Medicine, Kyoto University, Kyoto, Japan. [3]Department of Pediatrics, Hirosaki University Graduate School of Medicine, Hirosaki, Japan. [4]Laboratory of DNA Information Analysis, Human Genome Center, Institute of Medical Science, The University of Tokyo, Tokyo, Japan. [5]Department of Hematology/Oncology, Gunma Children's Medical Center, Shibukawa, Japan. [6]Laboratory of Sequence Analysis, Human Genome Center, Institute of Medical Science, The University of Tokyo, Tokyo, Japan. [7]Department of Pediatrics, Nagoya University Graduate School of Medicine, Nagoya, Japan. [8]Department of Pediatrics, St. Luke's International Hospital, Tokyo, Japan. [9]Department of Pediatrics, Hiroshima University Graduate School of Biomedical Sciences, Hiroshima, Japan. [10]Department of Pediatrics, Graduate School of Medicine, University of Toyama, Toyama, Japan. [11]Division of Neonatology, National Center for Child Health and Development, Tokyo, Japan. [12]Human Health Sciences, Graduate School of Medicine, Kyoto University, Kyoto, Japan. [13]Department of Pediatrics, Kagoshima City Hospital, Kagoshima, Japan. [14]Department of Hematology and Oncology, Children's Medical Center, Japanese Red Cross Nagoya First Hospital, Nagoya, Japan. [15]Department of Pediatrics, School of Medicine, Institute of Medical, Pharmaceutical and Health Sciences, Kanazawa University, Kanazawa, Japan. [16]Functional Genomics, Cancer Research Center, Sheba Medical Center, Tel Hashomer and Tel Aviv University, Tel Aviv, Israel. [17]These authors contributed equally to this work. [18]These authors jointly directed this work. Correspondence should be addressed to S.O. (sogawa-tky@umin.ac.jp) or E.I. (eturou@cc.hirosaki-u.ac.jp).

Received 3 May; accepted 19 August; published online 22 September 2013; corrected after print 30 October 2013; doi:10.1038/ng.2759

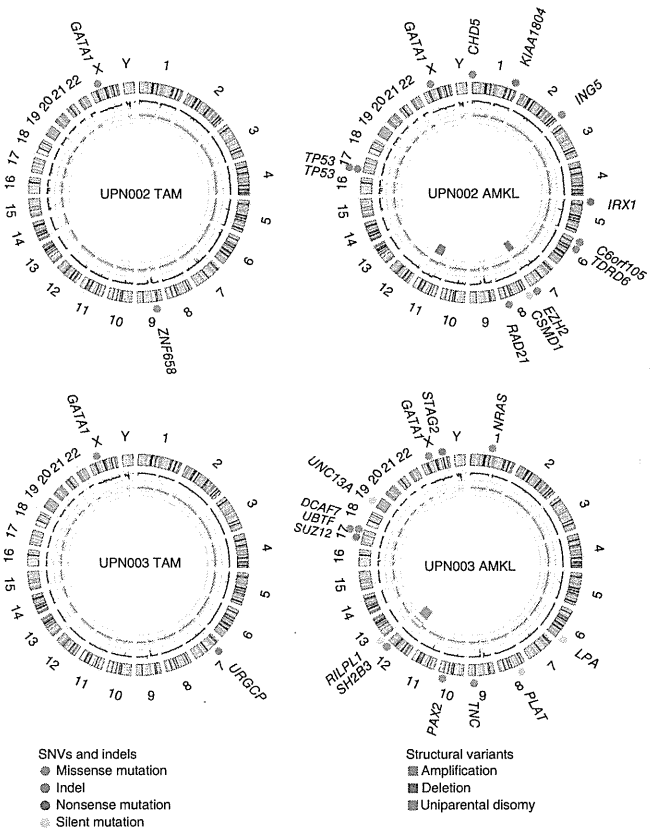

Figure 1 Representative Circos plots of paired TAM and DS-AMKL cases. Locations of somatic mutations, including of missense, frameshift, nonsense and silent mutations (colored circles), are indicated. Total (black) and allele-specific (red and green for alleles showing relatively larger and smaller copy numbers, respectively) genomic copy numbers, as well as somatic structural variants (colored bars), are indicated in the inner circle. Sample IDs are shown within each plot; plots were created with Circus[53].

we confirmed 411 single-nucleotide variants (SNVs) and 17 small nucleotide insertions and deletions (indels) by Sanger sequencing and/or deep resequencing (**Supplementary Fig. 1** and **Supplementary Table 2**). We detected only a few structural variants, including deletion, amplification and uniparental disomy, in the TAM and DS-AMKL genomes (**Fig. 1** and **Supplementary Fig. 3**). The mean number of validated somatic mutations in DS-AMKL samples (71 or 0.023 mutations/Mb) was twice the number observed in TAM samples (36 or 0.012 mutations/Mb) (**Supplementary Fig. 1a**). Mutation numbers in samples from both phases were substantially lower than in most other cancers (**Supplementary Fig. 4**), although differences in mutation rates could partly be affected by different definitions and algorithms for mutation calling. The spectrum of mutations was over-represented by C-to-T and G-to-A transitions in both TAM and DS-AMKL samples, resembling the mutational spectra in gastric and colorectal cancers[13] and in other blood cancers (**Supplementary Fig. 1b**)[14,15]. We unmasked the details of clonal evolution and expansion leading to AMKL through the use of deep sequencing of individual mutations detected by combined whole-genome and whole-exome sequencing (**Fig. 2** and **Supplementary Table 2**). Intratumoral heterogeneity was evident at initial diagnosis with TAM and in the AMKL phase in all cases (**Supplementary Fig. 5**). In UPN001, UPN002 and UPN004, AMKL evolved from one of the major subclones in the TAM phase with a shared *GATA1* mutation, as reported previously in relapsed acute myeloid leukemia (AML) in adults (**Fig. 2a,b,d**)[15]. In contrast, UPN003 showed a unique pattern of clonal evolution, in which AMKL originated from a minor subclone in the TAM phase that was totally unrelated to the predominant clone in terms of somatic mutations, with no mutation shared by both phases, and carried an independent *GATA1* mutation (**Fig. 2c**). In both scenarios, progression to AMKL seemed to be accompanied by many additional mutations, including common driver mutations that were absent in the original TAM population, indicating a multistep process of leukemogenesis.

Exome sequencing

We further investigated non-silent mutations by whole-exome sequencing of additional samples to generate a full registry of driver mutations that are relevant to the development of TAM and subsequent progression to AMKL (**Supplementary Fig. 6** and **Supplementary Table 1**). We detected *GATA1* mutations in all TAM and DS-AMKL cases, indicating sufficient sensitivity in our whole-exome analysis. In total, we confirmed 26 and 81 non-silent somatic mutations identified in the exome analysis of 15 TAM and 14 DS-AMKL samples, respectively, with 3 *GATA1* mutations common to both phases (**Supplementary Table 3**). The mean number of non-silent mutations was significantly higher in DS-AMKL samples (5.8; range of 1–11) than in TAM samples (1.7; range of 1–5) ($P = 0.0002$) (**Fig. 3a**). Of the 107 mutations, 84 were single-nucleotide substitutions that were mostly within coding sequences, except for 4 splice-site mutations. We also observed predominantly C-to-T and G-to-A transitions for non-silent substitutions (**Supplementary Fig. 7**). The remaining mutations were frameshift ($n = 21$) or non-frameshift ($n = 2$) indels, most frequently involving *GATA1* ($n = 13$). One individual with DS-AMKL (UPN004) had no SNVs or indels (**Fig. 3a**), but copy number analysis identified a large deletion at 16q involving the *CTCF* locus (**Supplementary Fig. 3**), suggesting that the alteration of *CTCF* could be a driver event in this case. Therefore, at least one additional genetic lesion other than *GATA1* mutation was detected in our whole-exome sequencing, despite the low frequency of leukemic cells appearing to show the morphology of immature megakaryoblasts (blast percentage) in many cases, which is a known characteristic of DS-AMKL samples[16,17]. Whole-exome sequencing results suggested the presence of intratumoral heterogeneity in the majority of DS-AMKL cases (**Fig. 3b**).

Spectrum of recurrent mutations in DS-AMKL

Recurrently affected genes are of primary interest in identifying driver mutations. Whereas *GATA1* was the only recurrent mutational target in TAM samples, an additional eight genes were recurrently mutated in the DS-AMKL samples, including *RAD21*, *STAG2*, *NRAS*, *CTCF*, *DCAF7*, *EZH2*, *KANSL1* and *TP53* (**Table 1**). These genes are expressed in a wide variety of hematopoietic compartments, including in both myeloid and lymphoid cells, except for *EZH2*, whose expression is largely confined to $CD34^+$ cells[18] (**Supplementary Fig. 8**). We also found that these genes were expressed in DS-AMKL cells at similar levels to common hematopoietic genes[19], although we did not observe significant difference in their expression levels in DS-AMKL and non-DS-AMKL cells (**Supplementary Fig. 9**).

We then performed targeted deep sequencing of these 8 genes in an extended set of 109 samples (including 29 samples in 25 discovery cases) consisting of 41 TAM, 49 DS-AMKL and 19 non-DS-AMKL samples (**Supplementary Tables 1** and **4**). We also included additional genes in targeted sequencing that were either functionally related to the above eight genes or were mutated only in single cases but had been previously reported to be mutated in DS-AMKL (*JAK3*) or other myeloid neoplasms (*SH2B3*, *SUZ12*, *SRSF2* and *WT1*), together with other common mutational targets in adult myeloid malignancies

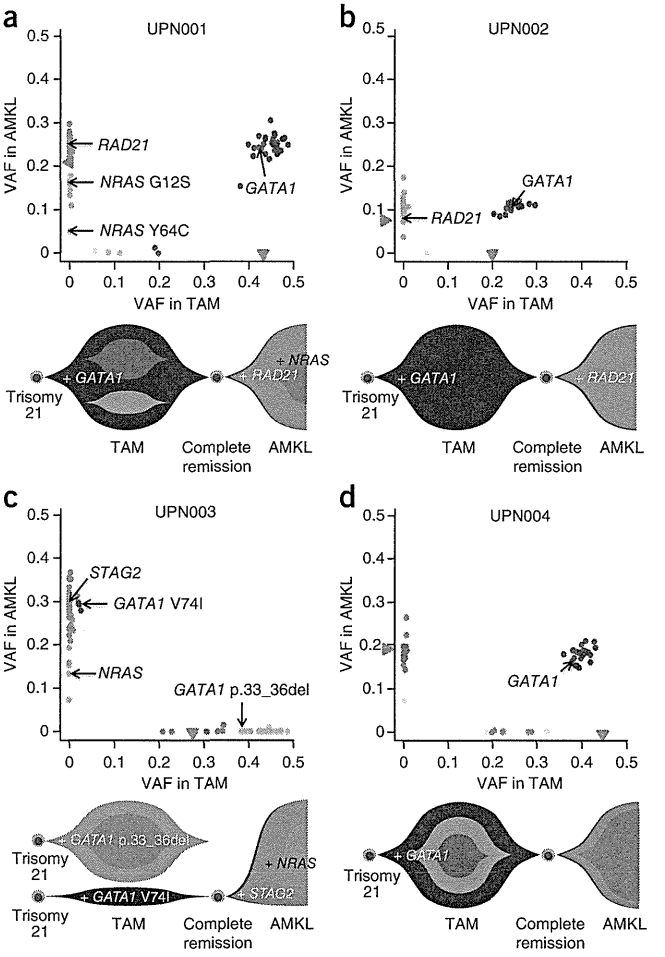

Figure 2 Clonal evolution of Down syndrome–related myeloid disorders. (**a–d**) Observed VAFs of validated mutations listed in **Supplementary Table 2** in both TAM and AMKL phases are shown in diagonal plots (top) for UPN001 (**a**), UPN002 (**b**), UPN003 (**c**) and UPN004 (**d**), where VAFs of genes on the X chromosome in male cases or in regions of uniparental disomy were halved. Half the value of the blast percentage, which corresponds to the allele frequency of a heterozygous mutation distributed in all tumor cells, is also shown by a red arrowhead, except for UPN003 AMKL, for which clinical data were not available. Driver mutations including in *GATA1*, *STAG2*, *RAD21* and *NRAS* are indicated by black arrows. Predicted chronological behaviors of different leukemia subclones are depicted below each diagonal plot. Distinct mutation clusters are indicated by color. In UPN001, UPN002 and UPN004, founding clones of TAM shown in blue became dominant in the AMKL samples, in which some subsequent subclones evolved through the serial acquisition of SNVs. In contrast, in UPN003, a subclone in the TAM phase (blue) and not the founding clone of TAM (aqua) became dominant in the AMKL sample. VAFs of some mutations were higher than for *GATA1* but seem to be actually equivalent to it given the error range of PCR-based deep sequencing.

(**Supplementary Fig. 10** and **Supplementary Tables 5** and **6**). We also analyzed by RT-PCR two recurrent fusion genes previously reported in non-DS-AMKL cases, *RBM15-MKL1* (*OTT-MAL*)[20,21] and *CBFA2T3-GLIS2* (refs. 22,23).

Mutations of cohesin and associated molecules

Major components of the cohesin complex, including *RAD21* and *STAG2*, were frequent targets of gene mutations in DS-AMKL (**Table 1**). Including an additional mutation in *NIPBL*, 8 of the 14 discovery DS-AMKL cases (57%) had a mutated cohesin or associated component (**Supplementary Table 3**). Cohesin is a multiprotein complex consisting of 4 core components, including the SMC1, SMC3, RAD21 and STAG proteins[24,25]. In concert with several functionally associated proteins, such as the NIPBL and ESCO proteins, cohesin is engaged in the cohesion of newly replicated sister chromatids by forming a ring-like structure[25], preventing their premature separation before late anaphase. Cohesin has also been implicated in post-replicative DNA repair and long-range regulation of gene expression[26–30]. Targeted deep sequencing confirmed recurrent mutations and deletions in all core cohesin components (*STAG2*, *RAD21*, *SMC3* and *SMC1A*) and in *NIPBL* in 26 of 49 DS-AMKL cases (53%) but in none of the 41 TAM cases, although 2 non-DS-AMKL cases (11%) had *STAG2* mutations (**Fig. 4a,b** and **Supplementary Tables 7** and **8**). Strikingly, all mutations and deletions in different cohesin components were completely mutually exclusive, suggesting that cohesin function was the common target of these mutations. All but one *STAG2* mutation (encoding a p.Arg370Gln substitution) was either a nonsense, frameshift or splice-site change (**Fig. 4a,b**, **Supplementary Figs. 11** and **12a**, and **Supplementary Table 7**). Similarly, 6 of 9 *RAD21* mutations were heterozygous nonsense or frameshift alterations. Four of the five mutations in *NIPBL*, *SMC1A* and *SMC3* were also nonsense or splice-site changes causing abnormal exon skipping (**Fig. 4a** and **Supplementary Table 7**). Thus, most of these mutations were thought to result in premature truncation, leading to loss of cohesin function. The leukemogenic mechanism of mutated cohesin components is still elusive; some studies have implicated aneuploidy caused by cohesin dysfunction in oncogenic actions[31]. However, DS-AMKL cases have been characterized by a largely normal karyotype[32]. We found no significant difference in the frequency of aneuploidy between cases with mutated and wild-type cohesin in the current DS-AMKL cohort. Many cases with mutated cohesin had completely normal karyotypes, except for constitutive trisomy 21, arguing against the hypothesis that aneuploidy has a major role in the pathogenesis of cohesin-mutated DS-AMKL (**Fig. 5a**).

CTCF mutations

Given the high frequency of cohesin mutations, new recurrent *CTCF* mutations were of particular interest because the functional interaction of cohesin and CTCF proteins has been of emerging interest in the long-range regulation of gene expression[26,30,33,34]. CTCF is a zinc-finger protein implicated in diverse regulatory functions, including transcriptional activation and/or repression, insulation, formation of chromatin barrier, imprinting and X-chromosome inactivation[35]. CTCF binds to target sequence elements and blocks the interaction of enhancers and promoters through DNA loop formation (insulator activity)[36], and several lines of evidence suggest that cohesin occupies CTCF-binding sites to contribute to the long-range regulation of gene expression by participating in the formation and stabilization of a repressive loop[26,37]. *CTCF* was mutated or deleted in ten DS-AMKL cases (20%), one TAM case (2%) and four non-DS-AMKL cases (21%), with seven mutations representing nonsense, frameshift or splice-site changes and an additional six alterations representing deletions resulting in the loss of protein function (**Fig. 4a,b**, **Supplementary Figs. 11** and **12b**, and **Supplementary Tables 7** and **8**). To our knowledge, this is the first report of frequent recurrent *CTCF* mutations in cancer, although rare mutations (occurring in approximately 2% of cases) have recently been reported in breast cancer sequencing[38].

Mutations in epigenetic regulators

EZH2, which encodes a catalytic subunit of the Polycomb repressive complex 2 (PRC2) that is responsible for di- and trimethylation of histone H3 lysine 27 (H3K27)[39], is another recurrent mutational target in DS-AMKL (**Table 1**). Inactivating mutations in *EZH2* have

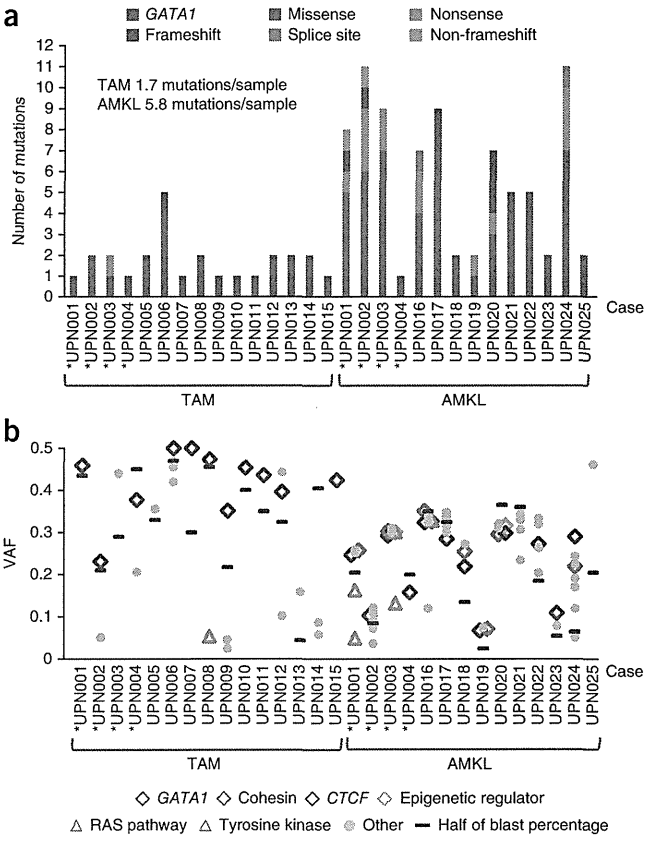

Figure 3 Somatic mutations detected by whole-exome sequencing of Down syndrome–related myeloid disorders. (**a**) Number of validated somatic mutations in 25 individuals with TAM and DS-AMKL identified by whole-exome sequencing. Paired samples are indicated by asterisks. The mutation rates per phase are given. (**b**) VAFs of individual mutations determined by deep sequencing, with VAFs adjusted for genomic copy numbers. Long indels of >3 bp were excluded from the analysis because their VAFs were difficult to accurately estimate. The VAF for each sample estimated on the basis of blast percentage is indicated by a purple horizontal bar.

been reported in up to 13% of myelodysplastic syndromes and related chronic myeloid neoplasms[40]. Although rarely mutated in adult AML[41], *EZH2* represents one of the most frequently mutated and deleted genes in childhood AMKL, as we identified mutations or deletions in 16 of 49 DS-AMKL cases (33%) and in 3 of 19 non-DS-AMKL cases (16%) (**Fig. 4a,b**, **Supplementary Fig. 12c** and **Supplementary Tables 7** and **8**). No other PRC2 components were mutated, except for *SUZ12*, which was mutated in a single DS-AMKL case (**Fig. 4a** and **Supplementary Table 7**). Although frequent mutations in other epigenetic regulators, including in *TET2*, *IDH1* or *IDH2*, *DNMT3A* and *ASXL1*, are cardinal features of myeloid neoplasms in adults, we rarely found these mutations in DS-AMKL and non-DS-AMKL cases, only identifying occasional *DNMT3A* ($n = 1$), *ASXL1* ($n = 1$) and *BCOR* ($n = 2$) mutations in DS-AMKL (**Fig. 4a**).

KANSL1 (encoding KAT8 regulatory NSL complex subunit 1; also known as MSL1V1 or NSL1) represents a new recurrent mutational target in human cancer (**Table 1**), although haploinsufficiency of *KANSL1* through germline deletions or mutations has been implicated in a congenital disease known as 17q21.31 microdeletion syndrome (MIM 610443)[42,43]. We found heterozygous mutations in *KANSL1* in three DS-AMKL and three non-DS-AMKL cases, and most of these mutations were nonsense or frameshifts, leading to loss of protein function (**Fig. 4a** and **Supplementary Table 7**). KANSL1 protein is necessary and sufficient for the activity of the KAT8 (MOF) histone acetyltransferase complex, which is engaged in the acetylation of histone H4 lysine 16 (H4K16), leading to transcriptional activation. Loss of acetylation of H4K16 has been reported to be a common hallmark of human cancer, and other histone acetyltransferases for H4K16 have been reported to form recurrent fusion partners in leukemia, including MOZ and MORF[44], suggesting a role for compromised H4K16 acetylation by *KANSL1* mutations in leukemogenesis. Of interest, KANSL1 is also responsible for the acetylation of the TP53 tumor suppressor that is important for TP53-dependent transcriptional activation[45]. KAT8 also interacts with a histone H3 lysine 4 (H3K4) methyltransferase, MLL, and the interaction of MLL and KAT8 complexes facilitates the cooperative recruitment of both complexes to gene promoters and enhances transcription initiation at target genes[45]. Thus, impaired TP53 function and/or deregulated expression of MLL gene targets could also contribute to leukemogenesis by *KANSL1* mutations.

Table 1 Recurrently mutated genes other than *GATA1* in DS-AMKL samples in whole-exome sequencing

Gene	Mutation type	RefSeq	Amino acid change	Nucleotide change	Sample (UPN) number
CTCF	Splice site	NM_006565	p.Gly318_splice	c.953–2A>G	016
CTCF	Frameshift	NM_006565	p.Asn314fs	c.940_941insAC	020
DCAF7	Missense	NM_005828	p.Leu340Phe	c.1018C>T	001
DCAF7	Missense	NM_005828	p.Leu340Phe	c.1018C>T	003
EZH2	Frameshift	NM_004456	p.710_716del	c.2129_2148delATCACAGGATAGGTATTTTT	001
EZH2	Missense	NM_004456	p.Arg25Gln	c.74G>A	002
KANSL1	Frameshift	NM_001193466	p.Arg720fs	c.2159_2160insCG	020
KANSL1	Nonsense	NM_001193466	p.Arg462*	c.1384C>T	024
NRAS	Missense	NM_002524	p.Gly12Ser	c.34G>A	001
NRAS	Missense	NM_002524	p.Tyr64Cys	c.191A>G	001
NRAS	Missense	NM_002524	p.Gly12Ala	c.35G>C	003
RAD21	Nonsense	NM_006265	p.Arg139*	c.415A>T	001
RAD21	Frameshift	NM_006265	p.374_375del	c.1120_1124delTCTTT	002
RAD21	Missense	NM_006265	p.Leu611Arg	c.1832T>G	018
RAD21	Nonsense	NM_006265	p.Arg65*	c.193C>T	024
STAG2	Nonsense	NM_001042750	p.Arg604*	c.1810C>T	003
STAG2	Nonsense	NM_001042750	p.Arg216*	c.646C>T	019
STAG2	Frameshift	NM_001042750	p.Asn863fs	c.2588_2589insT	020
TP53	Nonsense	NM_000546	p.Glu68*	c.202G>T	002
TP53	Non-frameshift	NM_000546	p.157_162del	c.469_486delGTCCGCGCCATGGCCATC	002

Other mutations in DS-AMKL

RAS pathway mutations are common in hematopoietic malignancies and other human cancers but have not to our knowledge been described in DS-AMKL. In the current cohort, we identified RAS pathway

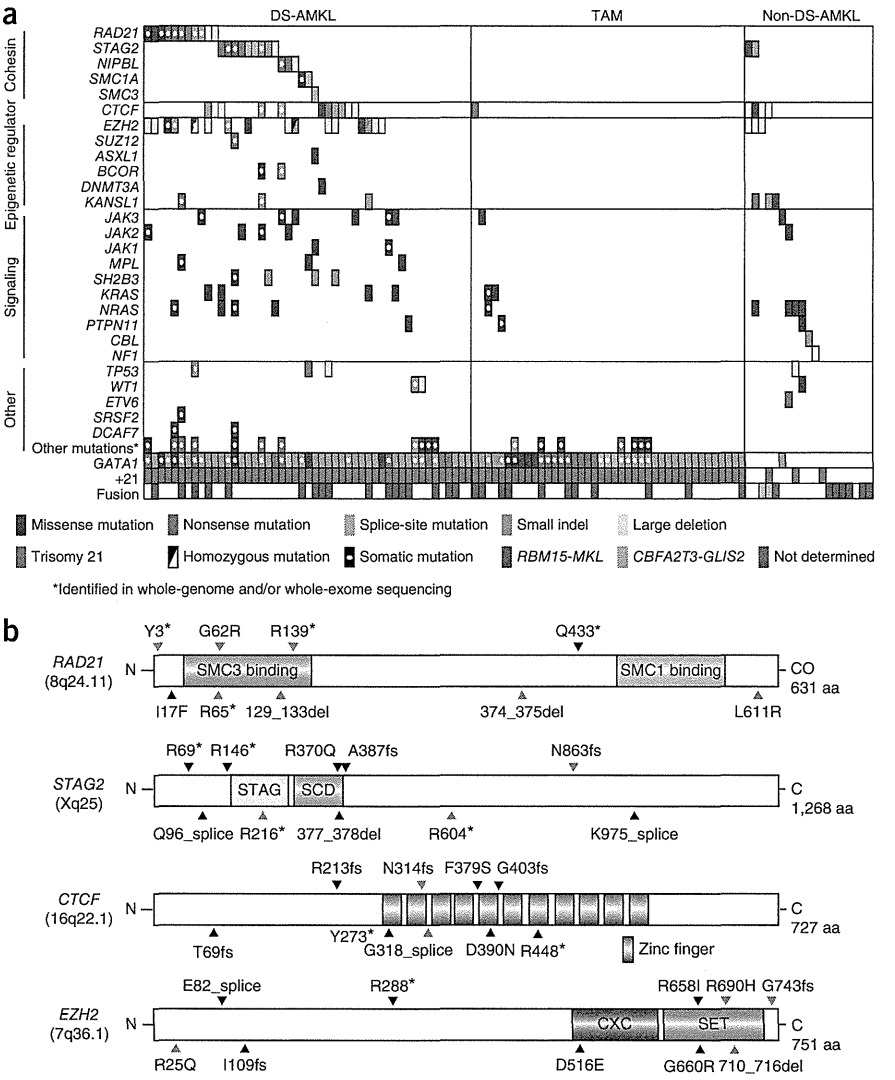

Figure 4 Driver mutations in Down syndrome–related myeloid disorders and non-DS-AMKL. (**a**) Driver mutations in 109 samples of 49 DS-AMKL, 41 TAM and 19 non-DS-AMKL cases. Types of mutations are distinguished by color. Each sample is also described in **Supplementary Table 12**. (**b**) Distribution of RAD21, STAG2, CTCF and EZH2 alterations. Alterations encoded by confirmed somatic mutations are indicated by red arrowheads.

mutations in the *NRAS*, *KRAS*, *PTPN11*, *NF1* and *CBL* genes in 8 DS-AMKL cases (16%) and 6 non-DS-AMKL cases (32%), but these mutations were rarely found in TAM cases (n = 3; 7%) (**Fig. 4a**). Tyrosine kinase and cytokine receptor mutations were also common in DS-AMKL. We found mutations in *JAK1*, *JAK2*, *JAK3*, *MPL* or *SH2B3* (*LNK*) in 17 DS-AMKL cases (35%) but rarely in TAM (n = 1) and non-DS-AMKL (n = 2) cases. We found no *FLT3* mutations in our cohort. The identified mutations were largely mutually exclusive. We found *JAK2* mutations in 4 DS-AMKL cases and 1 non-DS-AMKL case, including mutations encoding p.Val617Phe (n = 2), p.Leu611Ser (n = 1), p.Arg683Ser (n = 1) and p.Arg867Gln (n = 1); of these, *JAK2* mutations encoding p.Arg683Ser and p.Arg867Gln substitutions have been reported in acute lymphoblastic leukemia (ALL)[46,47] but not in myeloid malignancies[8,46]. Thus, we re-evaluated the diagnosis of AMKL in both UPN097 (p.Arg683Ser) and UPN023 (p.Arg867Gln), in whom the initial diagnosis of AMKL was strongly supported by typical surface marker expression of CD41, CD41b, CD117, CD13, CD33, CD34 and CD36 in UPN097 and of CD7, CD13, CD34, CD41a and CD42b in UPN023, together with characteristic cytomorphology. Similarly, the mutation encoding p.Leu611Ser was reported in both ALL[48] and polycythemia vera[49]. Thus, it seems that some *JAK2* mutations are involved in both myeloid and lymphoid leukemogenesis. As reported previously[10,11], *TP53* mutations were found in approximately 10% of DS-AMKL cases. Two identical somatic mutations found in the *DCAF7* gene (encoding p.Leu340Phe) might be interesting because the DCAF7 protein interacts with the DYRK1a kinase encoded within the Down syndrome critical region on chromosome 21 (ref. 50). DCAF7 has been shown to interact with DYRK1a through its N-terminal or C-terminal region, and the p.Leu340Phe substitution identified in our study was also located in the C-terminal domain. However, no additional mutation was detected in the extended cohort; therefore, the relevance of *DCAF7* remains to be determined.

Allelic burden of major recurrent mutations relative to *GATA1* mutations

We assessed intratumoral heterogeneity and the clonal origin of mutations by calculating the variant allele frequency (VAF) of each mutation relative to that of the *GATA1* mutation using deep sequencing. Mutations in cohesin components, *CTCF* and *EZH2* showed comparable VAFs to *GATA1* mutations (**Fig. 5b**), suggesting their role in the early stage of DS-AMKL development. In contrast, RAS pathway and other tyrosine kinases and cytokine receptor mutations showed significantly lower VAFs than corresponding *GATA1* mutations (P = 0.0001) (**Fig. 5b**), indicating that they are more likely to represent subclonal mutations, which were typically preceded by mutations in cohesin components, *CTCF* and *EZH2* and were involved in the evolution of multiple DS-AMKL subclones. Although RAS and JAK pathways activated by gene mutations represent potentially druggable targets and several promising compounds are currently available, this observation may largely preclude the efficient use of such compounds in eradicating founding DS-AMKL clones.

Distinct genetic features of Down syndrome– and non–Down syndrome–related AMKL

Despite their morphological similarities, both forms of AMKL in childhood are characterized by distinctive genetic features. According to the current study and a recent report of integrated analysis of non-DS-AMKL[22], *GATA1* mutations and trisomy 21 are less common in non-DS-AMKL than in DS-AMKL cases (**Fig. 4a** and **Supplementary Table 9**). In our series, DS-AMKL was characterized by high frequencies of mutations in the cohesin complex, *EZH2* and other epigenetic regulators, as well as in JAK family kinases, which were less

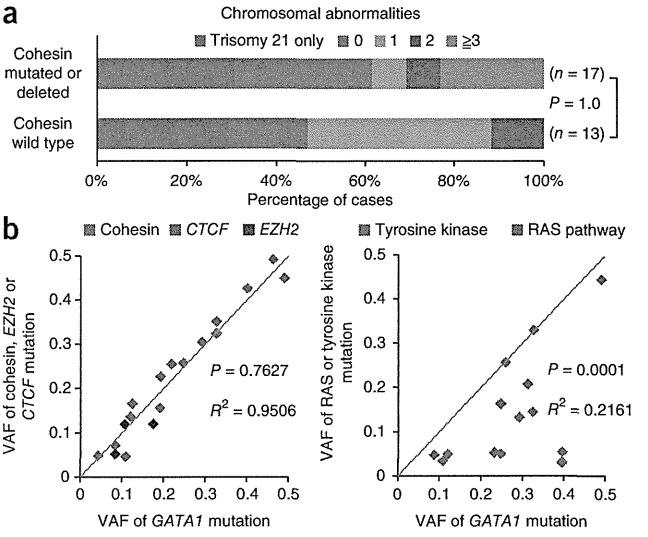

Figure 5 Relationship of cohesin mutations with karyotypes and comparison of mutation loads between major gene targets in DS-AMKL and *GATA1*. (**a**) The number of chromosomal abnormalities is compared between cases with and without cohesin mutations or deletions for DS-AMKL cases. Zero signifies chromosomal abnormalities without change in chromosome count, such as partial amplification or deletion of the chromosomal region or balanced translocation. (**b**) Diagonal plots of copy number–adjusted VAFs comparing coexisting *GATA1* and other pathway mutations, including cohesin, *CTCF*, *EZH2*, tyrosine kinase and the RAS pathway mutations, as indicated by color.

common mutational targets in non-DS-AMKL. Previous studies identified recurrent *CBFA2T3-GLIS2* and *RBM15-MKL* gene fusions in non-DS-AMKL, which were found in 27% and 15.2% of non-DS-AMKL cases, respectively[22,51], whereas these fusions were not detected in DS-AMKL cases in another report (n = 10 cases)[23]. Similarly, in the current cohort, RT-PCR analysis identified 2 *CBFA2T3-GLIS2* and 3 *RBM15-MKL* fusion genes in 19 non-DS-AMKL cases but not in TAM and DS-AMKL cases (**Fig. 4a** and **Supplementary Table 10**), illustrating the genetic differences between DS-AMKL and non-DS-AMKL. In addition, our RNA sequencing of the current cases (n = 17) (**Supplementary Table 11**) also showed no *CBFA2T3-GLIS2* and *RBM15-MKL* fusions.

DISCUSSION

Whole-genome and/or whole-exome analyses and follow-up targeted sequencing identified several new aspects of the pathogenesis of Down syndrome–related myeloid proliferation. First, the initial TAM phase was characterized by a paucity of somatic mutations. The mean number of non-silent mutations per sample (1.7; range of 1–5) was surprisingly small compared with that reported in other human cancers (**Supplementary Fig. 13**), in line with a recent report that identified 1.2 (range of 1–2) mutations per sample by whole-exome sequencing in 5 TAM samples[52]. In addition to reporting a low somatic mutation frequency in their initial TAM phase, Nikolaev *et al.*[52] also reported accumulation of somatic mutations (including single cases of *SMC3* and *EZH2* mutation) during progression from TAM to DS-AMKL. Excluding common *GATA1* mutations, we identified no other recurrent mutations, with only 0.7 non-silent mutations per case, indicating that TAM could be caused by a single acquired *GATA1* mutation in addition to constitutive trisomy 21.

Intratumoral heterogeneity was evident not only in the DS-AMKL phase but also at the initial diagnosis of TAM, and subsequent DS-AMKL originated from one of the multiple subclones present in the TAM phase, usually representing the progeny of the largest subpopulation. In most cases, the DS-AMKL clone was accompanied by newly acquired driver mutations not shared by the original TAM population, generating a unique landscape of gene mutations in DS-AMKL, which was characterized by high mutational frequencies in cohesin or *CTCF* (65%), other epigenetic regulators (45%), and RAS or signal-transducing molecules (47%) (**Fig. 4a**). Tumor recurrence or evolution has not to our knowledge been characterized by the distinct gene mutations in greater detail than in the present study. In total, 44 of the 49 DS-AMKL cases had additional mutations beyond those in *GATA1* (**Fig. 4a**), even though there was a clear limitation on capturing mutations using the targeted sequencing approach.

The very high frequency of cohesin (53%) and *EZH2* (33%) mutations and deletions in DS-AMKL but not in TAM or non-DS-AMKL cases was noteworthy because the reported mutation rates of cohesin and *EZH2* in adult AML and other human cancers remain approximately 10% (refs. 14,40,41), underscoring a major role for these mutations in the pathogenesis of DS-AMKL. The leukemogenic mechanism of mutated cohesin remains elusive, and frequent *CTCF* mutations also need further evaluation to characterize their possible cooperative role with cohesin mutations[26,30,33,34]. To our knowledge, *KANSL1* mutations have not been reported previously and represent a new recurrent mutational target in human cancer, although their functional impact on AMKL development remains unknown. Evaluation of the allelic burden of these mutations by deep sequencing disclosed a clonal hierarchy among different driver mutations in which clonal mutations in cohesin, *CTCF* and epigenetic regulators frequently preceded subclonal mutations in RAS and signal transduction molecules.

In conclusion, Down syndrome–related myeloid proliferation is shaped by multiple rounds of acquisition of new mutations and clonal selection, which are initiated by a *GATA1* mutation in the TAM phase and further driven by mutation in cohesin or *CTCF*, *EZH2* or other epigenetic regulators, and RAS or signal-transducing molecules, leading to AMKL. DS-AMKL and non-DS-AMKL showed similar phenotypes but had distinct genetic features, which may underlie their different clinical characteristics.

URLs. European Genome-phenome Archive (EGA), https://www.ebi.ac.uk/ega/; EBCall, https://github.com/friend1ws/EBCall; Catalogue of Somatic Mutations in Cancer (COSMIC), http://cancer.sanger.ac.uk/cancergenome/projects/cosmic/; PubMed, http://www.ncbi.nlm.nih.gov/pubmed/; UCSC Genome Browser, http://genome.ucsc.edu/; Integrative Genomics Viewer, http://www.broadinstitute.org/igv/; DNACopy, http://biostatistics.oxfordjournals.org/content/5/4/557.full.pdf; Genomon-fusion (in Japanese), http://genomon.hgc.jp/rna/.

METHODS

Methods and any associated references are available in the online version of the paper.

Accession codes. Sequencing data have been deposited in the European Genome-phenome Archive (EGA) under accession EGAS00001000546.

Note: Any Supplementary Information and Source Data files are available in the online version of the paper.

ACKNOWLEDGMENTS

We thank Y. Mori, M. Nakamura, O. Hagiwara and N. Mizota for their technical assistance. This work was supported by the Research on Measures for Intractable

Diseases Project and Health and Labor Sciences Research grants (Research on Intractable Diseases) from the Ministry of Health, Labour and Welfare, by Grants-in-Aid from the Ministry of Health, Labor and Welfare of Japan and KAKENHI (22134006, 23249052, 23118501, 23390266 and 25461579) and by the Japan Society for the Promotion of Science (JSPS) through the Funding Program for World-Leading Innovative Research and Development on Science and Technology (FIRST Program), initiated by the Council for Science and Technology Policy (CSTP) and research grants from the Japan Science and Technology Agency CREST.

AUTHOR CONTRIBUTIONS

Y.O., Y. Shiraishi, A.S.-O., K.C., H.T. and S.M. performed bioinformatics analyses of the resequencing data. M.S., A.S.-O., Y. Sato, A.H. and H.M. performed microarray experiments and analyses. R.K. and A.H. performed RT-PCR analyses. M.P., K. Terui, R.W., D.H., K.N., H.K., K. Tsukamoto, S.A., K. Kawakami, K. Kato, R.N., S.I., Y.H., S.K. and E.I. collected specimens and were involved in planning the project. K.Y., T.T., H.S., Y.N. and N.S. processed and analyzed genetic materials, prepared the library and performed sequencing. K.Y., T.T., Y.O., A.K. and S.O. generated figures and tables. E.I. and S.O. led the entire project. K.Y. and S.O. wrote the manuscript. All authors participated in discussions and interpretation of the data and results.

COMPETING FINANCIAL INTERESTS

The authors declare no competing financial interests.

1. Khan, I., Malinge, S. & Crispino, J. Myeloid leukemia in Down syndrome. *Crit. Rev. Oncog.* **16**, 25–36 (2011).
2. Massey, G.V. *et al.* A prospective study of the natural history of transient leukemia (TL) in neonates with Down syndrome (DS): Children's Oncology Group (COG) study POG-9481. *Blood* **107**, 4606–4613 (2006).
3. Muramatsu, H. *et al.* Risk factors for early death in neonates with Down syndrome and transient leukaemia. *Br. J. Haematol.* **142**, 610–615 (2008).
4. Klusmann, J.H. *et al.* Treatment and prognostic impact of transient leukemia in neonates with Down syndrome. *Blood* **111**, 2991–2998 (2008).
5. Xu, G. *et al.* Frequent mutations in the *GATA-1* gene in the transient myeloproliferative disorder of Down syndrome. *Blood* **102**, 2960–2968 (2003).
6. Wechsler, J. *et al.* Acquired mutations in *GATA1* in the megakaryoblastic leukemia of Down syndrome. *Nat. Genet.* **32**, 148–152 (2002).
7. Walters, D.K. *et al.* Activating alleles of *JAK3* in acute megakaryoblastic leukemia. *Cancer Cell* **10**, 65–75 (2006).
8. Malinge, S. *et al.* Activating mutations in human acute megakaryoblastic leukemia. *Blood* **112**, 4220–4226 (2008).
9. Blink, M. *et al.* Frequency and prognostic implications of *JAK 1–3* aberrations in Down syndrome acute lymphoblastic and myeloid leukemia. *Leukemia* **25**, 1365–1368 (2011).
10. Hama, A. *et al.* Molecular lesions in childhood and adult acute megakaryoblastic leukaemia. *Br. J. Haematol.* **156**, 316–325 (2012).
11. Malkin, D., Brown, E.J. & Zipursky, A. The role of p53 in megakaryocyte differentiation and the megakaryocytic leukemias of Down syndrome. *Cancer Genet. Cytogenet.* **116**, 1–5 (2000).
12. Hussein, K. *et al.* MPL^{W515L} mutation in acute megakaryoblastic leukaemia. *Leukemia* **23**, 852–855 (2009).
13. Greenman, C. *et al.* Patterns of somatic mutation in human cancer genomes. *Nature* **446**, 153–158 (2007).
14. Welch, J.S. *et al.* The origin and evolution of mutations in acute myeloid leukemia. *Cell* **150**, 264–278 (2012).
15. Ding, L. *et al.* Clonal evolution in relapsed acute myeloid leukaemia revealed by whole-genome sequencing. *Nature* **481**, 506–510 (2012).
16. Creutzig, U. *et al.* Diagnosis and management of acute myeloid leukemia in children and adolescents: recommendations from an international expert panel. *Blood* **120**, 3187–3205 (2012).
17. Swerdlow, S.H., Jaffe, E.S. & International Agency for Research on Cancer & World Health Organization *WHO Classification of Tumours of Haematopoietic and Lymphoid Tissues* (International Agency for Research on Cancer, Lyon, France, 2008).
18. Wu, C. *et al.* BioGPS: an extensible and customizable portal for querying and organizing gene annotation resources. *Genome Biol.* **10**, R130 (2009).
19. Bourquin, J.P. *et al.* Identification of distinct molecular phenotypes in acute megakaryoblastic leukemia by gene expression profiling. *Proc. Natl. Acad. Sci. USA* **103**, 3339–3344 (2006).
20. Mercher, T. *et al.* Involvement of a human gene related to the *Drosophila spen* gene in the recurrent t(1;22) translocation of acute megakaryocytic leukemia. *Proc. Natl. Acad. Sci. USA* **98**, 5776–5779 (2001).
21. Ma, Z. *et al.* Fusion of two novel genes, *RBM15* and *MKL1*, in the t(1;22)(p13;q13) of acute megakaryoblastic leukemia. *Nat. Genet.* **28**, 220–221 (2001).
22. Gruber, T.A. *et al.* An inv(16)(p13.3q24.3)-encoded CBFA2T3-GLIS2 fusion protein defines an aggressive subtype of pediatric acute megakaryoblastic leukemia. *Cancer Cell* **22**, 683–697 (2012).
23. Thiollier, C. *et al.* Characterization of novel genomic alterations and therapeutic approaches using acute megakaryoblastic leukemia xenograft models. *J. Exp. Med.* **209**, 2017–2031 (2012).
24. Gruber, S., Haering, C.H. & Nasmyth, K. Chromosomal cohesin forms a ring. *Cell* **112**, 765–777 (2003).
25. Nasmyth, K. & Haering, C.H. Cohesin: its roles and mechanisms. *Annu. Rev. Genet.* **43**, 525–558 (2009).
26. Wendt, K.S. *et al.* Cohesin mediates transcriptional insulation by CCCTC-binding factor. *Nature* **451**, 796–801 (2008).
27. Ström, L. *et al.* Postreplicative formation of cohesion is required for repair and induced by a single DNA break. *Science* **317**, 242–245 (2007).
28. Watrin, E. & Peters, J.M. The cohesin complex is required for the DNA damage–induced G2/M checkpoint in mammalian cells. *EMBO J.* **28**, 2625–2635 (2009).
29. Dorsett, D. *et al.* Effects of sister chromatid cohesion proteins on *cut* gene expression during wing development in *Drosophila*. *Development* **132**, 4743–4753 (2005).
30. Parelho, V. *et al.* Cohesins functionally associate with CTCF on mammalian chromosome arms. *Cell* **132**, 422–433 (2008).
31. Solomon, D.A. *et al.* Mutational inactivation of *STAG2* causes aneuploidy in human cancer. *Science* **333**, 1039–1043 (2011).
32. Forestier, E. *et al.* Cytogenetic features of acute lymphoblastic and myeloid leukemias in pediatric patients with Down syndrome: an iBFM-SG study. *Blood* **111**, 1575–1583 (2008).
33. Rubio, E.D. *et al.* CTCF physically links cohesin to chromatin. *Proc. Natl. Acad. Sci. USA* **105**, 8309–8314 (2008).
34. Stedman, W. *et al.* Cohesins localize with CTCF at the KSHV latency control region and at cellular c-myc and H19/Igf2 insulators. *EMBO J.* **27**, 654–666 (2008).
35. Ohlsson, R., Bartkuhn, M. & Renkawitz, R. CTCF shapes chromatin by multiple mechanisms: the impact of 20 years of CTCF research on understanding the workings of chromatin. *Chromosoma* **119**, 351–360 (2010).
36. Phillips, J.E. & Corces, V.G. CTCF: master weaver of the genome. *Cell* **137**, 1194–1211 (2009).
37. Wendt, K.S. & Peters, J.M. How cohesin and CTCF cooperate in regulating gene expression. *Chromosome Res.* **17**, 201–214 (2009).
38. Cancer Genome Atlas Network. Comprehensive molecular portraits of human breast tumours. *Nature* **490**, 61–70 (2012).
39. Cao, R. *et al.* Role of histone H3 lysine 27 methylation in Polycomb-group silencing. *Science* **298**, 1039–1043 (2002).
40. Ernst, T. *et al.* Inactivating mutations of the histone methyltransferase gene *EZH2* in myeloid disorders. *Nat. Genet.* **42**, 722–726 (2010).
41. Patel, J.P. *et al.* Prognostic relevance of integrated genetic profiling in acute myeloid leukemia. *N. Engl. J. Med.* **366**, 1079–1089 (2012).
42. Koolen, D.A. *et al.* Mutations in the chromatin modifier gene *KANSL1* cause the 17q21.31 microdeletion syndrome. *Nat. Genet.* **44**, 639–641 (2012).
43. Zollino, M. *et al.* Mutations in *KANSL1* cause the 17q21.31 microdeletion syndrome phenotype. *Nat. Genet.* **44**, 636–638 (2012).
44. Yang, X.J. The diverse superfamily of lysine acetyltransferases and their roles in leukemia and other diseases. *Nucleic Acids Res.* **32**, 959–976 (2004).
45. Li, X., Wu, L., Corsa, C.A., Kunkel, S. & Dou, Y. Two mammalian MOF complexes regulate transcription activation by distinct mechanisms. *Mol. Cell* **36**, 290–301 (2009).
46. Bercovich, D. *et al.* Mutations of *JAK2* in acute lymphoblastic leukaemias associated with Down's syndrome. *Lancet* **372**, 1484–1492 (2008).
47. Mullighan, C.G. *et al.* JAK mutations in high-risk childhood acute lymphoblastic leukemia. *Proc. Natl. Acad. Sci. USA* **106**, 9414–9418 (2009).
48. Kratz, C.P. *et al.* Mutational screen reveals a novel JAK2 mutation, L611S, in a child with acute lymphoblastic leukemia. *Leukemia* **20**, 381–383 (2006).
49. Nussenzveig, R.H. *et al.* Detection of *JAK2* mutations in paraffin marrow biopsies by high resolution melting analysis: identification of L611S alone and in *cis* with V617F in polycythemia vera. *Leuk. Lymphoma* **53**, 2479–2486 (2012).
50. Miyata, Y. & Nishida, E. DYRK1A binds to an evolutionarily conserved WD40-repeat protein WDR68 and induces its nuclear translocation. *Biochim. Biophys. Acta* **1813**, 1728–1739 (2011).
51. de Rooij, J.D. *et al.* *NUP98/JARID1A* is a novel recurrent abnormality in pediatric acute megakaryoblastic leukemia with a distinct *HOX* gene expression pattern. *Leukemia* doi:10.1038/leu.2013.87 (27 March 2013).
52. Nikolaev, S.I. *et al.* Exome sequencing identifies putative drivers of progression of transient myeloproliferative disorder to AMKL in infants with Down Syndrome. *Blood* **122**, 554–561 (2013).
53. Krzywinski, M. *et al.* Circos: an information aesthetic for comparative genomics. *Genome Res.* **19**, 1639–1645 (2009).

ONLINE METHODS

Subjects and samples. Genomic DNA from 84 individuals with Down syndrome–related myeloid disorders (41 samples from the TAM phase and 49 from the AMKL phase) and 19 with non-DS-AMKL were analyzed by whole-genome and/or whole-exome and/or targeted deep sequencing. In six cases with Down syndrome–related myeloid disorders, samples were collected from both the TAM and AMKL phases. RNA sequencing was also performed for 12 of the 49 DS-AMKL cases and for 5 additional DS-AMKL cases. RNA samples were also available for RT-PCR analysis from 30 cases with TAM, 32 cases with DS-AMKL and 15 cases with non-DS-AMKL. Written informed consent was obtained from each subject's parents before sample collection (**Supplementary Note**). This study was approved by the Ethics Committees of the University of Tokyo according to the Helsinki convention. *GATA1* mutations were detected by Sanger sequencing of all TAM and DS-AMKL samples according to the previously described procedure[5]. Detailed information on subjects and samples is provided in **Supplementary Tables 1, 4, 11** and **12**. Tumor DNA was extracted from bone marrow– or peripheral blood–derived mononuclear cells at diagnosis. Genomic DNA samples from peripheral blood from subjects in remission or from nail tissues at diagnosis were used as germline controls. Genomic DNA was extracted using a QIAamp DNA Blood Mini kit and a QIAamp DNA Investigator kit (Qiagen). Total RNA was extracted using the RNeasy kit (Qiagen) with RNase-free DNase (Qiagen).

Whole-genome sequencing. DNA samples were processed for whole-exome sequencing using NEBNext DNA sample Prep Reagent (New England Biolabs) according to the modified Illumina protocol. Sequence data were generated on the Illumina HiSeq 2000 platform in 100-bp paired-end reads. Data processing and variant calling were performed as described previously[54]. All candidate variants were validated by deep sequencing.

Validation and quantitative measurements of the frequencies of mutant alleles by deep sequencing. Individual mutation sites were amplified by genomic PCR using primers tagged with NotI cleavage sites and subjected to high-throughput sequencing as described previously[55], except that target DNA was not pooled. Deep sequencing was performed using the MiSeq or HiSeq 2000 platform. Data processing was performed according to the previously described method with minor modifications[55]. Briefly, each read was aligned to a set of PCR-amplified target sequences using BLAT[56], and dichotomic variant alleles were differentially enumerated. For indels, individual reads were first aligned to each of the wild-type and indel sequences and then assigned to the one to which better alignment was obtained in terms of the number of matched bases. Each SNV and indel whose VAF in the tumor sample was equal to or greater than 2.0% and significantly higher than the frequency in the germline sample was adopted as a somatic mutation. The error size for estimated VAFs was evaluated by assuming binomial distributions in deep sequencing, which were confirmed by observed allele frequencies at heterozygous SNPs in normal DNA samples (**Supplementary Fig. 14a**), in which the variance (σ^2) ranged from $4.0–11.0 \times 10^{-4}$ (**Supplementary Fig. 14b**).

Clustering analysis of mutations. To identify the chronological behavior of the structure of the tumor subpopulation for the TAM and AMKL phases, somatic mutations detected in both phases by whole-genome sequencing were clustered according to their VAFs as measured by deep sequencing. Copy number–adjusted deep sequencing data, in which the VAFs of genes on the X chromosome in male cases or in regions of uniparental disomy were halved, were subjected to unsupervised clustering. Six mutations located in amplified or deleted genomic regions were excluded from the analysis. Long indels of >3 bp, except for those affecting key genes such as *GATA1* and *RAD21*, and mutations in repetitive regions were excluded from the analysis because their VAFs could tend to be underestimated.

All validated mutations were grouped into three categories according to the following criteria: (i) mutations found only in TAM (VAF in AMKL < 0.02), (ii) mutations found only in AMKL (VAF in TAM < 0.02) and (iii) mutations found in both TAM and AMKL (VAF in TAM > 0.02 and VAF in AMKL > 0.02). Clustering of mutations in each category was performed using Mclust, provided as an R package, on the basis of the VAFs of the mutations in the TAM and AMKL phases, where one-dimensional clustering of mutations in categories (i) and (ii) was performed on the basis of the homoscedastic model and two-dimensional clustering was performed for mutations in category (iii) on the basis of the ellipsoidal model. The most appropriate number of clusters was determined by using the Bayesian information criterion (BIC) score. Singleton points identified by this algorithm were regarded as outliers. Clonal subpopulations within tumors were also evaluated by kernel density analysis (**Supplementary Fig. 5**), where we drew kernel density estimate plots for the VAFs of validated variants using the density function in R.

Whole-exome sequencing and detection of somatic mutations. Exome capture was performed using SureSelect Human All Exon V3 or V4 (Agilent Technologies) or the TruSeq Exome Enrichment kit (Illumina). Enriched exome fragments were then subjected to massively parallel sequencing using the Genome Analyzer IIx or HiSeq 2000 platform (Illumina). Candidate somatic mutations were detected using our in-house pipeline EBCall (Empirical Bayesian mutation Calling; see URLs)[57]. All candidates were validated by Sanger sequencing or independent deep sequencing.

PCR-based targeted deep sequencing. Deep sequencing of *DCAF7*, *EED*, *JAK1*, *JAK3*, *KANSL1*, *SH2B3*, and *SUZ12* was performed using the primers tagged with NotI cleavage sites whose sequences are listed in **Supplementary Table 6**. Data processing and variant calling were performed as described previously[58]. All candidate variants were validated by Sanger sequencing or independent deep sequencing using non-amplified DNA.

Targeted deep sequencing. In total, 39 gene targets were exhaustively examined for mutations in all 109 cases using deep sequencing (**Supplementary Table 5**). Genomic DNA (1–1.5 μg) from bone marrow–derived mononuclear cells or peripheral blood was enriched for target exons using a SureSelect custom kit (Agilent Technologies) designed to capture all of the coding exons from the 39 target genes, and high-throughput sequencing was performed on the enriched targets using the HiSeq 2000 platform with a standard 100-bp paired-end read protocol. Sequencing reads were aligned to hg19 using Burrows-Wheeler Aligner (BWA) version 0.5.8 with default parameters. The allele frequencies of SNVs and indels were calculated at each genomic position by enumerating the relevant reads with SAMtools[59]. Initially, all variants showing VAF > 0.02 were extracted and annotated using ANNOVAR[60] for further consideration if they were found in >6 reads out of >10 total reads and appeared in both plus- and minus-strand reads. For the cases for which no germline DNA was available, relevant somatic mutations were called by eliminating the following entries, unless they were registered in the Catalogue of Somatic Mutations in Cancer (COSMIC) v60 (ref. 61) or reported as somatic mutations in PubMed: (i) synonymous variants and those having ambiguous (unknown) annotations, (ii) known SNPs in public and private databases, including dbSNP131, the 1000 Genomes Project as of 23 November 2010 and our in-house database, (iii) sequencing or mapping errors, (iv) all missense SNVs with allele frequencies of 0.45–0.55 and (v) variants localized to duplicated regions found in SegDups of the UCSC Genome Browser. To eliminate sequencing errors in category (iii), we excluded all variants found in 31 normal Japanese samples at, on average, allele frequency > 0.25. Mapping errors were removed by visual inspection with the Integrative Genomics Viewer browser[62]. All candidate variants were validated by Sanger sequencing or independent deep sequencing.

Calculation of copy numbers for target exons. Letting $d_j^{i,s}$ be the sequencing depth at the ith nucleotide of the jth exon in sample s, the standardized depth of the jth exon is calculated as

$$D_j^s = k_s \sum_i d_i^{j,s}$$

where k_s is determined to satisfy

$$k_0 = \sum_j D_j^s$$

for a fixed constant k_0 (for example, $k_0 = 1$). The correlation coefficient ($R = R^{s,t}$) between two vectors D_i^s and D_i^t was calculated, where D_i^s and D_i^t represent the depth for a given sample (sample s) and each of the 443

samples (sample t), analyzed for other projects, with completely normal copy numbers in array–comparative genomic hybridization (aCGH; $t = 1, 2, 3,\ldots, 443$), respectively, through which a total of m_0 (= 12) control samples showing the largest R values were selected (T_m; $m = 1, 2, 3,\ldots, m_0$) and used for copy number calculation. The copy number of the ith target exon of sample s (Cn_i^s) was calculated as

$$Cn_i^s = D_i^s / \hat{D}_i^s$$

where $\hat{D}_i^s$ was calculated by averaging m_0 samples by

$$\hat{D}_i^s = \sum_{m=1}^{m_0} D_i^{Tm} / m_0$$

Copy numbers were calculated for exons with mean depth of >500. Circular binary segmentation was also used to identify discrete copy number segments using DNACopy (see URLs); segmented copy number ($\widehat{Cn_i^s}$) was defined for the ith exon of sample s. The distribution of $\widehat{Cn_i^s}$ was calculated for all samples, and exons showing $|\widehat{Cn_i^s} - E(\widehat{Cn_i^s})| > 4$ s.d. were considered to have copy number losses or gains.

Screening for *CBFA2T3-GLIS2* and *RBM15-MKL1* fusion genes. *CBFA2T3-GLIS2* and *RBM15-MKL1* fusion genes were screened by RT-PCR[22,63]. Primer sequences are given in **Supplementary Table 13**. PCR amplification was performed by 40 cycles at 94 °C for 2 min, 60 °C for 30 s and 68 °C for 1 min, followed by denaturation at 94 °C for 2 min and extension at 68 °C for 7 min.

SNP array analyses. All tumor samples subjected to whole-exome sequencing were also analyzed for copy number alterations using SNP arrays (Affymetrix GeneChip Human Mapping 250K NspI Array or Genome-Wide Human SNP Array 6.0) as described previously[10,64,65].

RT-PCR analysis of *STAG2* and *CTCF* transcripts. To confirm abnormal splicing of *CTCF* in UPN016 and UPN071 and that of *STAG2* in UPN067, RT-PCR were performed using cDNA derived from each subject, with cDNA from CMK11-5 (DS-AMKL–derived cell line with no known mutations in both genes) used as a control (**Supplementary Fig. 11**). Primer sequences are given in **Supplementary Table 14**. Total RNA (1 μg) was subjected to reverse transcription using M-MLV reverse transcriptase (Invitrogen) according to the manufacturer's instructions. Electrophoresis was performed using Experion (Bio-Rad).

RNA sequencing. Detailed information on samples is provided in **Supplementary Table 11**. Library preparation and sequencing were performed as described previously[54]. Fusion transcripts were detected using Genomon-fusion.

Gene expression analysis of recurrently mutated genes. Expression data for the recurrently mutated genes in whole-exome sequencing were retrieved from the BioGPS database[18] for normal hematopoietic cells, including whole bone marrow, CD33$^+$ myeloid cells, CD34$^+$ cells, CD19$^+$ B cells and CD4$^+$ T cells, and from published data[19] and our RNA sequencing data for DS-AMKL samples.

Statistical analysis. The number of non-silent mutations identified by whole-exome sequencing in TAM and DS-AMKL samples (**Fig. 2a**) and the number of chromosome abnormalities in DS-AMKL cases with and without cohesin mutations or deletions (**Fig. 5a**) were compared using the Mann-Whitney U test. The difference in VAF between two mutations (**Fig. 5b**) was tested by Wilcoxon signed-rank test.

54. Sato, Y. *et al.* Integrated molecular analysis of clear-cell renal cell carcinoma. *Nat. Genet.* **45**, 860–867 (2013).
55. Yoshida, K. *et al.* Frequent pathway mutations of splicing machinery in myelodysplasia. *Nature* **478**, 64–69 (2011).
56. Kent, W.J. BLAT—the BLAST-like alignment tool. *Genome Res.* **12**, 656–664 (2002).
57. Shiraishi, Y. *et al.* An empirical Bayesian framework for somatic mutation detection from cancer genome sequencing data. *Nucleic Acids Res.* **41**, e89 (2013).
58. Sakaguchi, H. *et al.* Exome sequencing identifies secondary mutations of *SETBP1* and *JAK3* in juvenile myelomonocytic leukemia. *Nat. Genet.* **45**, 937–941 (2013).
59. Li, H. *et al.* The Sequence Alignment/Map format and SAMtools. *Bioinformatics* **25**, 2078–2079 (2009).
60. Wang, K., Li, M. & Hakonarson, H. ANNOVAR: functional annotation of genetic variants from high-throughput sequencing data. *Nucleic Acids Res.* **38**, e164 (2010).
61. Forbes, S.A. *et al.* COSMIC: mining complete cancer genomes in the Catalogue of Somatic Mutations in Cancer. *Nucleic Acids Res.* **39**, D945–D950 (2011).
62. Robinson, J.T. *et al.* Integrative genomics viewer. *Nat. Biotechnol.* **29**, 24–26 (2011).
63. Torres, L. *et al.* Acute megakaryoblastic leukemia with a four-way variant translocation originating the *RBM15-MKL1* fusion gene. *Pediatr. Blood Cancer* **56**, 846–849 (2011).
64. Nannya, Y. *et al.* A robust algorithm for copy number detection using high-density oligonucleotide single nucleotide polymorphism genotyping arrays. *Cancer Res.* **65**, 6071–6079 (2005).
65. Yamamoto, G. *et al.* Highly sensitive method for genomewide detection of allelic composition in nonpaired, primary tumor specimens by use of Affymetrix single-nucleotide-polymorphism genotyping microarrays. *Am. J. Hum. Genet.* **81**, 114–126 (2007).